Review

Early Warning Method and Fire Extinguishing Technology of Lithium-Ion Battery Thermal Runaway: A Review

Kuo Wang [1], Dongxu Ouyang [2,*], Xinming Qian [1,*], Shuai Yuan [1], Chongye Chang [1], Jianqi Zhang [1] and Yifan Liu [1]

1 State Key Laboratory of Explosion Science and Technology, Beijing Institute of Technology, Beijing 100084, China
2 College of Safety Science and Engineering, Nanjing Tech University, Nanjing 210009, China
* Correspondence: ouyang11@mail.ustc.edu.cn (D.O.); qsemon@bit.edu.cn (X.Q.)

Abstract: Lithium-ion batteries (LIBs) are widely used in electrochemical energy storage and in other fields. However, LIBs are prone to thermal runaway (TR) under abusive conditions, which may lead to fires and even explosion accidents. Given the severity of TR hazards for LIBs, early warning and fire extinguishing technologies for battery TR are comprehensively reviewed in this paper. First, the TR reaction mechanism and hazards of LIBs are discussed. Second, the TR early warning and monitoring methods of LIBs are summarized in five aspects consisting of acoustic, heat, force, electricity, and gas. In addition, to reduce the fire and explosion hazards caused by the TR of LIBs, the highly efficient extinguishing agents for LIBs are summarized. Finally, the early warning technology and fire extinguishing agent are proposed, which provides a reference for the hazard prevention and control of energy storage systems.

Keywords: lithium-ion battery; thermal runaway; early warning method; fire extinguishing agent

1. Introduction

In order to solve the problem of the traditional energy shortage and environmental pollution, the goal of carbon neutralization and carbon peak was put forward, namely "dual carbon target". Electrochemical energy storage is an important part of achieving the "dual carbon target", and lithium-ion batteries (LIBs) account for more than 93% of the electrochemical energy storage [1], which is growing with each passing year. However, with the continuous improvement in the energy density of LIBs, they face great challenges, as they are prone to fire and explosion under abusive conditions. The frequent occurrence of accidents has made the industry lose confidence and hindered the further development of LIBs.

In recent years, accidents caused by batteries have become increasingly apparent. According to incomplete statistics, there have been more than 60 fire accidents in battery power storage stations around the world in the past decade [2], and the accompanying safety risks and impacts are far more serious than those of new energy electric vehicles. From August 2017 to May 2019, more than 20 fire accidents occurred in South Korea [3], and all energy storage projects were suspended. On 19 April 2019, an explosion accident occurred in the battery storage facility of Arizona Public Service Company (APS), located in the McMicken substation (the United States), causing multiple firefighters to be injured, two of whom were seriously injured. The accident investigation found that white dendrites were growing on the surface of the carbon anode. These dendrites pierced the separator, thus causing battery thermal runaway (TR). The gas caused by the TR gathered in the energy storage facility, which was disturbed when the firefighter opened the door and the battery exploded. In this accident, although the fire extinguishing system (Novec 1230) was triggered, heat spread was not prevented. On 16 April 2021, a fire broke out in the south building of the Dahongmen Energy Storage Power Station in Fengtai District, Beijing. Dry

powder extinguishers were used to put out the fire, but the extinguished battery modules quickly reignited. In addition, two firefighters were killed, and one was seriously injured when the North Building exploded without warning. The endless safety accidents of LIBs also indicate a serious lack of early warning and efficient fire extinguishing technologies for LIBs. Table 1 lists several typical LIB safety accidents around the world in recent years.

Table 1. Several typical LIB safety accidents [4].

Date	Accident Reply	Battery Type and Energy Storage Capacity	Cause of Accident	Whether Early Warning and Fire Fighting Measures Are Taken
19 April 2019	An explosion occurred at the Arizona Public Service (APS) battery storage facility at the McMicken transformer Station, USA	Lithium nickel manganese cobalt (NCM), 2MWh	Internal defects of the battery, abnormal deposition and growth of lithium dendrite, and uncontrolled thermal combustible gas reaching the explosive limit	Novec 1230 a fully submerged extinguishing agent was used, which did not inhibit the TR transmission
6 April 2021	Fire and explosion of Hongcheng PV + energy storage system in South Chungching, South Korea	NCM, 10MWh	Insufficient battery over-current and over-voltage protection, poor operating environment (humidity and dust) and installation process	/
16 April 2021	An explosion has occurred at the Dahongmen DC optical Storage and Charging integrated power station project in Fengtai District, Beijing, China	lithium iron phosphate (LFP), 25MWh	Inflammable and explosive gas accumulation reaches the explosion limit	During installation and commissioning, the dry powder was used to extinguish the fire, but reignition occurred
30 July 2021	Fire in Megapack energy storage system in Tesla, Victoria, Australia	LFP, 450 MWh	The leakage of the cooling system leads to the short circuit of the battery, which leads to the occurrence and propagation of TR	During installation and commissioning, the monitoring system did not operate for 24 h, and the fault was not detected in time. Firefighting water was used to extinguish the fire
4 September 2021	Fire of Moss landing energy storage battery in California, USA	Unknown, 1200 MWh	Battery module overheating	During operation, a targeted sprinkler system was triggered to spray water on the affected modules, causing damage to 7% of the battery modules
18 April 2022	A fire broke out at an energy storage facility at a Salt River substation in Arizona, USA	Unknown, 40 MWh	The battery has internal defects	The internal sprinkler system has been running for four days, but it has not been completely extinguished, and the battery is still smoldering and smoking

Certain progress has been made in terms of the intrinsic safety and prevention and control technology of battery TR, for example, reducing battery heat generation (use safe electrolytes [5–8], high temperature resistant flame retardant separator [9,10], anode without lithium dendrites [11], thermally stable cathode [12], etc.) and controlling temperature rise (use phase change materials [13,14], optimize battery structure [15], adopt air cooling and liquid cooling technology [16,17], etc.). However, battery TR still often occurs due to improper use and abuse and even leads to fire and explosion, causing casualties and property losses [18–21]. Therefore, early warning of the occurrence of TR and preventing serious harm have become the key issues that need to be solved urgently, which means that early warning and efficient firefighting prevention measures must be implemented for TR.

TR of LIBs is usually caused by three abuse modes (mechanical abuse, electrical abuse, and thermal abuse) [22]. Due to abuse, a short circuit occurs inside the battery,

and the voltage and impedance change significantly; the internal materials of the battery react exothermically, generating a lot of heat, and the battery temperature rises rapidly. Representative gases (such as CO_2, H_2, CO, CH_4) are released and the battery expands. When the internal pressure exceeds the pressure that the safety valve can withstand, the safety valve cracks, and the gas and active substance particles are ejected and released [23]. Therefore, according to the characteristics of LIBs TR, multi-parameter safety early warnings based on "acoustic, heat, force, electricity, gas" and other aspects can be developed, and efficient and clean fire protection technology can be exploited. Active prevention, dynamic monitoring before TR, efficient fire extinguishing after TR, and a combination of prevention and elimination are effective means to reduce battery accidents and property losses. In this paper, the process and characteristics of TR are discussed in detail, and a comprehensive review of safety warning methods and efficient fire extinguishing is provided, which supplies possible directions for early safety warnings and efficient fire extinguishing of TR.
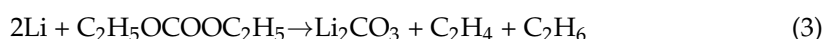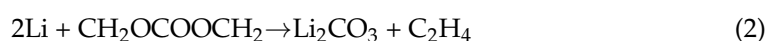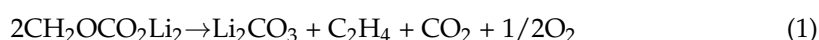
2. Thermal Runaway of Lithium-Ion Batteries

2.1. Mechanism and Process of Thermal Runaway

TR of LIBs is a phenomenon in which the battery temperature rises uncontrollably due to the exothermic chain reaction inside the battery cell [24]. The TR process can be divided into three stages: the first stage is the early stage of TR, when a chemical reaction occurs inside the battery to release heat and produce gas, and the internal pressure of the battery increases. The second stage is the TR period, when the safety valve is opened, and the flue gas is released. The third stage is the period of fire and explosion; combustibles spray through the safety valve and release a large amount of a high-temperature flammable and explosive mixture. The high-temperature mixture accumulates in a confined space and causes an explosion when encountering ignition sources.
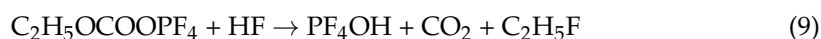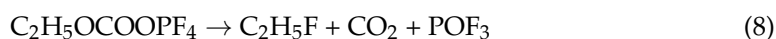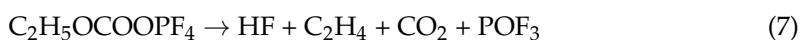
(1)　　Stage I: Early stage of TR

With the gradual increase in the battery temperature, TR occurs due to the decomposition of battery anode solid electrolyte interphase (SEI) film at 70–120 °C. The SEI film on the anode surface is not stable at high temperatures, which causes decomposition and exothermic reactions, and the battery temperature continues to rise. As the temperature rises to 120 °C, the anode material has a side reaction with the electrolyte. Due to the decomposition of the SEI film on the anode surface, the anode active material loses its protection, and the new graphite is exposed to organic solvents. Under the action of high temperatures, lithium embedded in the graphite anode reacts with the electrolyte. The chemical reaction equations are as follows [25]:

$$2CH_2OCO_2Li_2 \rightarrow Li_2CO_3 + C_2H_4 + CO_2 + 1/2O_2 \tag{1}$$

$$2Li + CH_2OCOOCH_2 \rightarrow Li_2CO_3 + C_2H_4 \tag{2}$$

$$2Li + C_2H_5OCOOC_2H_5 \rightarrow Li_2CO_3 + C_2H_4 + C_2H_6 \tag{3}$$

When the temperature rises to 120–140 °C, the separator begins to melt, and the voltage drops for a short time. The battery releases a lot of heat immediately after the internal short circuit. As the battery temperature rises to 200 °C, a large amount of organic flammable gas begins to be generated inside the LIBs. The chemical reaction equations of electrolyte decomposition at high temperatures are as follows [25]:

$$LiPF_6 + H_2O \rightarrow LiF + HF + POF_3 \tag{4}$$

$$C_2H_5OCOOC_2H_5 + PF_5 \rightarrow C_2H_5OCOOPF_4 + HF + C_2H_4 \tag{5}$$

$$C_2H_5OCOOC_2H_5 + PF_5 \rightarrow C_2H_5OCOOPF_4 + C_2H_5F \tag{6}$$

$$C_2H_5OCOOPF_4 \rightarrow HF + C_2H_4 + CO_2 + POF_3 \tag{7}$$

$$C_2H_5OCOOPF_4 \rightarrow C_2H_5F + CO_2 + POF_3 \tag{8}$$

$$C_2H_5OCOOPF_4 + HF \rightarrow PF_4OH + CO_2 + C_2H_5F \tag{9}$$

As the temperature continues to rise, the cathode material decomposes (different cathode materials have different decomposition temperatures as follows: $LiCoO_2$, 150 °C; $LiNi_xCo_yMn_zO_2$, 210 °C; $LiMn_2O_4$, 265 °C; and $LiFePO_4$, 310 °C [26]. Then, the cathode material reacts with the electrolyte, and the cathode reacts with the binder at high temperatures.

(2)   Stage II: TR occurrence period

At this stage, the battery is full of gas, and the internal pressure of the battery increases sharply. When the internal pressure of the battery reaches the set pressure of the safety valve, it is torn to release the internal gas and prevent the battery from exploding [27]. When the safety valve breaks, it is accompanied by a clear opening sound [28]. Subsequently, a large volume of flammable, explosive, and toxic gases are ejected, accompanied by some active substances and electrolyte vapors. These flammable substances are soon ignited at high temperatures.

(3)   Stage III: Fire and explosion occurrence

As the internal temperature of the battery continues to accumulate, the electrochemical reaction and thermal decomposition reaction intensify, the temperature rises rapidly, and the internal gas and pressure of the battery greatly increase. Although the overall relative positions of the tightly wound jelly roll remain unchanged, the separation phenomenon occurs in local areas, and the material structure of the inner layer of the core first deforms. After the safety valve is opened and released, the internal pressure of the battery is uneven, leading to the collapse of the electrode layers [29]. Then, the air gradually infiltrates into the battery and the collapse area expands, eventually causing TR. The TR fire behavior of LIBs is similar [30]. First, a large number of sparks are ejected, followed by a jet fire accompanied by solid particles. Then, the flame gradually turns to steady combustion, and continues to weaken. Finally, the combustibles burn out, and the flame goes out.

2.2. Hazard Characteristics of Battery Thermal Runaway

As shown in Figure 1, the hazard characteristics of single battery TR mainly include acoustic, heat, force, electricity, gas, etc. The typical hazard characteristics of TR of a single battery are discussed below. An extensive understanding of the characteristics of battery TR can guide the better realization of TR warnings and firefighting.

2.2.1. Thermal Runaway Acoustic Signal Characteristics of Lithium-Ion Batteries

LIBs are equipped with safety valves at the top, which allow batteries to expand internally when TR occurs. When the internal pressure exceeds the pressure that can be borne, the safety valve is opened to reduce pressure and avoid the occurrence of an explosion [31]. By monitoring the TR acoustic signal in the battery experimental cabin, it was found that the safety valve emits a sound at a specific frequency when it is opened. In the process of battery exhaust, there is a strong short shock wave in the acoustic signal, and the amplitude increased rapidly and then decreased exponentially [32]. Cheng et al. [33] found that the acoustic signal of the battery is similar at different times and temperatures. The acoustic signal characteristics can help determine whether the battery has TR.
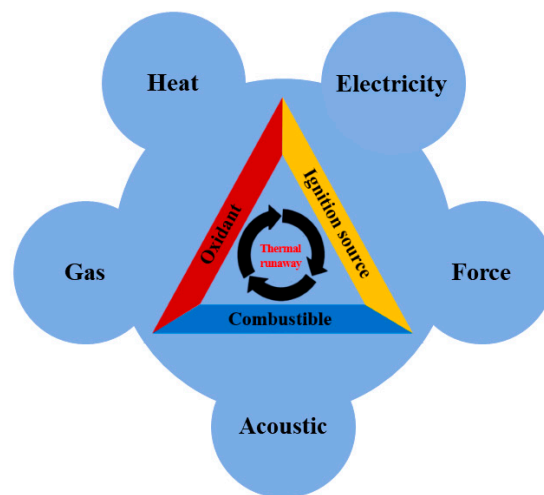
Figure 1. Hazard characteristics of battery TR.

2.2.2. Thermal Runaway Heat Generation of Lithium-Ion Batteries

The temperature rise rate of LIBs is determined by self-generated heat and heat dissipation [34], as shown in Equation (10). The increase in battery energy Q depends on the self-generated heat Q_{cell} and heat transfer intensity of the battery. Q_{cell} is the amount of heat generated by chemical reactions inside a battery as its temperature rises. Its calorific value is mainly composed of the electrochemical reaction heat Q_r, Joule heat Q_j generated by internal resistance, polarization heat Q_p generated by internal electrode caused by battery capacity or environmental change, and side reaction heat Q_{side} [35]. When the battery works in a normal environment, its heat production is mainly composed of Q_r, Q_j and Q_p, and when the battery is abused, serious side reactions occur inside the battery, producing a lot of Q_{side}.

$$Q = Q_{cell} - Q_{conv} - Q_{rad} \tag{10}$$

$$Q_{cell} = Q_r + Q_j + Q_p + Q_{side} \tag{11}$$

The heat transfer intensity depends on the heat convection Q_{conv} and heat radiation Q_{rad} of the battery [36].

$$Q_{conv} = hA(T_s - T) \tag{12}$$

$$Q_{rad} = \varepsilon\sigma A\left(T_s^4 - T^4\right) \tag{13}$$

where h is the thermal conductivity, A is the contact area, T_s is the surface temperature of the heater, T is the temperature on the boundary of the battery, ε is the emissivity, and σ is the Stefan-Boltzmann constant (5.67×10^{-8} W/(m^2 K^4)).

The battery also has thermal inertia. When the battery is in the process of charging and discharging, the internal heat production of the battery increases, and the internal temperature increases rapidly. Due to the existence of a heat conduction process, the external temperature change is relatively delayed. With the integrated use of batteries, thermal inertia between batteries increases exponentially, and the heat source inside the batteries disappears after power failure, but its heat conduction continues and is still very easy to cause TR. Thermal inertia is related to the battery discharge rate, discharge depth, and battery radius and greatly affects the thermal behavior and thermal characteristics of the battery during and after discharge. It is worth considering the early warning system design of LIBs.

2.2.3. Thermal Runaway Force Performance Changes of Lithium-Ion Batteries

In the initial stage of TR, the battery first increases the internal pressure due to gas generation. Mier et al. [37] studied the pressure dynamics during the TR process of 18,650 LIBs and found that the increase in the battery's internal pressure was consistent with the beginning of TR. When the internal pressure accumulates to the maximum extent that the safety valve can withstand, the battery internal pressure is reduced by jet release, but the pressure of the surrounding environment rapidly increases. Jhu et al. [38] used Vent Sizing Package 2 (VSP2) to measure the release pressure of 18,650 batteries' TR and found that the pressure swiftly rises, and the maximum pressure can reach 1565.9 psig (without the blowdown buffer tank). Zhao [39] found that external pressure was positively correlated with the total heat production of batteries' TR. In addition, the peak pressure was more similar to the total energy released by cells under different states of charge (SOC) [40].

2.2.4. Thermal Runaway Electricity Performance Changes of Lithium-Ion Batteries

Before battery TR, the voltage and resistance are disordered. The micropores of the internal Li^+ channel are closed, causing the Li^+ channel to be blocked, resulting in a sharp rise in the ohmic internal resistance of the battery under high-temperature conditions [41]. Zhong et al. [42] used an improved cone calorimeter to heat batteries in different SOCs. It was found that the voltage decreased before TR. The voltage of the battery drops sharply when the safety valve is opened, and TR occurs with flame ejection, but it increases slightly during the intervening period. According to research and analysis, the first sharp drop in voltage may be caused by the separator thermal contraction, and the cathode and anode have contacted at the edge of the original separator.

2.2.5. Thermal Runaway Gas Production of Lithium-Ion Batteries

LIBs are mostly used in enclosed or semi-enclosed spaces. Especially when large-capacity batteries are overcharged, a large amount of energy in the batteries cannot be effectively released, and flammable and explosive gases are easily accumulated [43]. LIBs usually produce a large number of flammable and toxic gases in the process of TR, such as CO, HF, SO_2, NO, and HCl. Larsson et al. [44] studied the fire heat generation and toxic gas release of commercial LFP batteries under different SOCs. The higher the SOC, the higher the peak value of the heat release rate. Toxic gas HF was found in all experiments, but POF_3 and PF_5 were not detected. Diaz et al. [45] used online Fourier Transform Infrared Spectroscopy (FTIR) and Ion Chromatography (IC) to quantitatively analyze the TR gas and evaluate its toxicity. The results showed that the main toxic components were HF, CF_2O, C_3H_4O, CO, CH_2O, HCl, and electrolytic solvent. In addition to the emission of fluorine-containing gas and electrolyte solvent evaporation, LIBs also produce other gases, such as H_2, CO_2, CH_4, C_2H_6, and C_2H_4 [46]. When the gas mixture is ejected from the safety valve, the speed of gas ejection may become turbulent and supersonic [47]. Furthermore, when the TR of LIBs occurs in a confined space and the combustible gas mixture released reaches the explosion limit, serious gas deflagration accidents occur, which is far more dangerous than battery fire. Wang et al. [48] studied the gas release of LIBs with different cathode materials during TR. The experimental results showed that the main components of gas production of NCM and LFP batteries were similar, but the explosion pressure test results showed that the explosion limit of gas released by LFP batteries was lower, the explosion over-pressure was larger, and the explosion index was higher. Therefore, the exhaust of the LFP battery was more harmful to fire and explosion than that of the NCM battery. The components of TR gas produced by LIBs with different cathode materials are shown in Table 2.

Table 2. TR gas components of LIBs with different cathode materials [48].

Vent Gas Composition (%)	H_2	CO	CO_2	CH_4	C_2H_4	C_2H_6	$n\text{-}C_4H_{10}$	Others
NCM111	20.81	14.82	42.91	5.88	8.11	1.57	3.16	2.73
NCM523	20.24	21.27	37.96	7.51	7.08	1.58	2.43	1.93
NCM622	15.48	20.07	41.09	10.56	6.47	2.45	1.87	2.02
NCM811	16.07	25.65	34.37	17.39	1.17	3.98	/	1.37
LFP	36.24	7.39	25.24	6.41	15.2	2.36	1.28	2.21

3. Early Warning Methods for Typical Lithium-Ion Batteries

The process of TR is usually accompanied by changes in acoustic, thermal properties, mechanical properties, electrical properties, gas generation, and so on. With the help of these changes, the occurrence, development, and severity of TR can be judged. If the battery TR is warned in advance by technical means, the firefighting challenge of LIBs will be reduced. At present, research on TR early warning technology for LIBs is mainly aimed at real-time monitoring of battery status, whether there is a failure, and the type of failure before TR or serious consequences caused by TR propagation so as to achieve early warning of TR and avoid further large-scale losses.

3.1. Safety Monitoring Method Based on Acoustic Signal

3.1.1. Ultrasonic Testing

Ultrasonic testing is a method for structural health monitoring and nondestructive evaluation and has been widely used in material characterization [49,50]. The application of ultrasonic monitoring in LIBs has also been widely studied. Davies et al. [51] detected the change in battery SOC through the time of flight (TOF) difference of ultrasound. A long-term cycle test shows that this technology can also be used to monitor the battery state of health (SOH). The research of Hsieh et al. [52] showed that ultrasonic technology can be used to monitor the geometric shape of a battery. Owen et al. [53] proposed that the battery temperature has a strong impact on the TOF, and the battery temperature is inferred through ultrasound to accurately predict the battery charging state at different magnifications.

There are two main methods for ultrasonic monitoring [54]: the first is the pulse-echo mode, where the ultrasonic signal is sent and received by the same transducer, as shown in Figure 2a. The essence of battery degradation is the variation of battery material characteristics (density and modulus, i.e., changes in the amount of lithium in the electrode [51]); this results in changes in ultrasonic impedance and velocity. The ultrasonic impedance Z of a material depends on its density ρ and ultrasonic velocity V. The relationship is shown in Equation (14):

$$Z = \rho^* V \tag{14}$$

Wu et al. [55] used the pulse echo method to continuously monitor the battery ultrasonic signal under the cycle process and overcharge test, and selected TOF reflects the propagation time of the ultrasonic signal inside the battery, as shown in Figure 2b, which indicates the change in ultrasonic velocity and/or thickness. The overcharge test shows that ultrasonic TOF is very sensitive to LIB expansion, which provides a potential indicator for LIB failure and TR. Similarly, the difference quotient of the TOF and swing amplitude (SA) of two adjacent measurements is calculated, and the difference quotient with the largest absolute value is selected as the threshold of TR warning for LIBs. Once the threshold is exceeded, the TR warning signal will be sent out [56].

$$\frac{\Delta TOF_{k-1}}{\Delta t_{k-1}} = \frac{TOF_k - TOF_{k-1}}{t_k - t_{k-1}} \tag{15}$$

$$\frac{\Delta SA_{k-1}}{\Delta t_{k-1}} = \frac{SA_k - SA_{k-1}}{t_k - t_{k-1}} \tag{16}$$

where subscripts k and $k-1$ represent the kth and $k-1$th measurement, respectively, and t represents time. Select the TOF and SA difference quotient results with the largest absolute values above and record them as $\left|\frac{\Delta TOF}{\Delta t}\right|_{max}$, $\left|\frac{\Delta SA}{\Delta t}\right|_{max}$.

The second is the through-transmission mode, as shown in Figure 2c, where the ultrasonic signal transmits through the object and is received by the second transducer. Appleberry et al. [57] defined the early indication of an abnormal battery state under over-charge conditions through ultrasonic signal change, which is the difference of 3.5 standard deviations between ultrasonic amplitude change and baseline average (baseline refers to the baseline average value of 30 cycles under normal parameters). The other is an emergency indication that the battery is about to experience TR under overcharge, which is 10 standard deviations from the mean of the ultrasonic baseline. The relevant deviations are shown in Figure 2d. The interaction between the ultrasound and the gas generated in the battery depends on the generation of bubbles in the battery. The generation of bubbles increases the TOF of ultrasound through the battery [58]. Similarly, the expansion of battery caused by gas production also causes an increase in the TOF. Most importantly, the formation of bubbles makes the ultrasound significantly scattered, and the amplitude of the signal significantly decreased.

3.1.2. Acoustical Signal

In the case of battery TR, the opening of the safety valve also makes a sound. Jin et al. [32] built a recognizer to identify the opening acoustic signal of the battery safety valve, collected and employed the acoustic signal to warn the TR of energy storage systems, as shown in Figure 2e. Lyu et al. [59] proposed a battery fault warning and location method based on a venting acoustic signal. An acoustic sensor was arranged in the energy storage cabin to collect the acoustic signal of the battery TR valve opening. Through the time of arrival (TOA), time difference of arrival (TDOA), and received signal strength (RSS) to locate the battery TR position, the maximum positioning error is only 0.1 m. The speed of sound propagation is 340 m/s, so it is easier to implement the early warning of battery TR by acoustic signal, and the acoustic signal sensor is cheap and has a wide range of applications. However, noise often exists in practical applications, which may interfere with the acoustic signal, leading to low accuracy in early warning technology.

3.2. Safety Monitoring Method Based on Thermal Signal

Temperature is the most important signal in the process of battery TR, which is a crucial parameter in determining TR. Monitoring and warning of the battery temperature is the most commonly used method. At present, the monitoring technologies that have been widely studied mainly include infrared thermal imaging, thermocouple, and optical fiber sensor. Battery temperatures can also be measured based on electrochemical parameters, which are reviewed in the next section. Battery TR is often caused by local overheating [60,61], and the temperature at different battery locations is not the same [62]. Therefore, accurate monitoring of battery temperature fluctuations and local overheating is very important for early warning of TR. Real-time monitoring and measurement of the temperature play a significant role in the TR early warning.
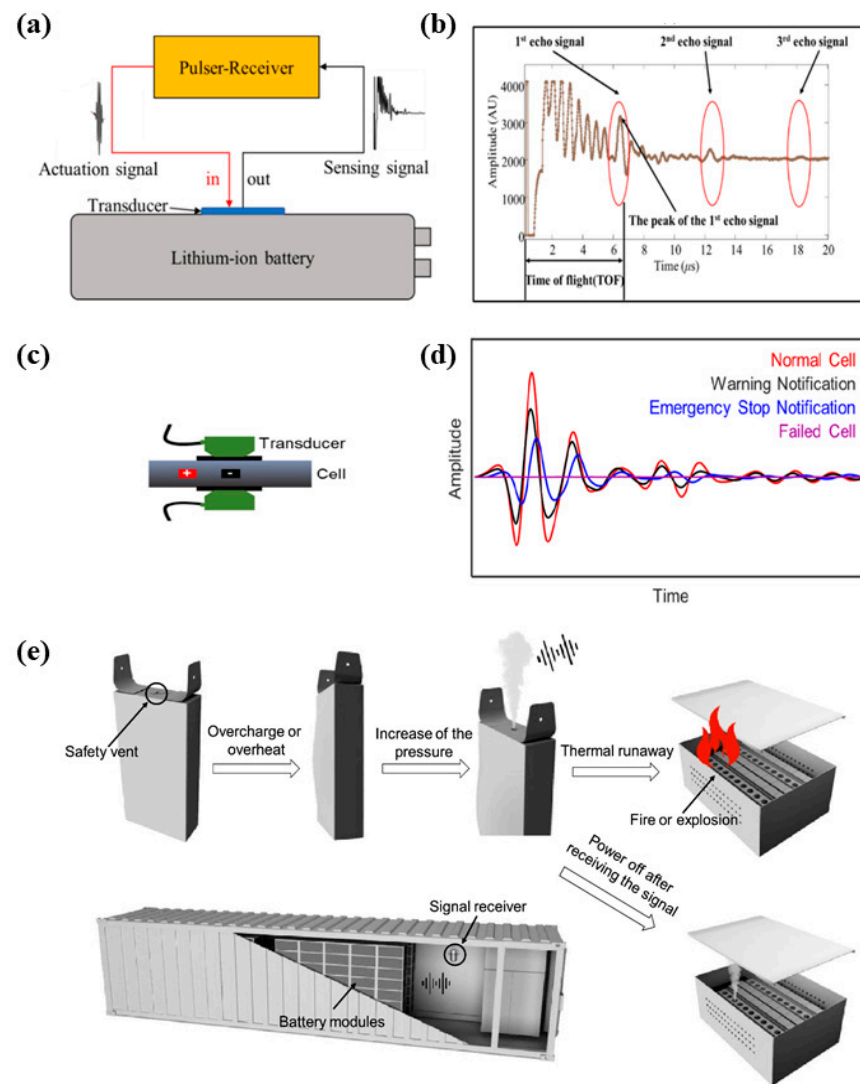
Figure 2. Acoustic safety monitoring method: (**a**) pulse-echo mode [54]; (**b**) propagation time of ultrasonic signal inside the battery [55]; (**c**) through-transmission mode [54]; (**d**) ultrasonic amplitude change [57]; (**e**) acoustic signal to warn the TR [32].

3.2.1. Infrared Thermal Imaging and Thermocouple

In recent years, infrared thermal imagers have been widely used to measure the surface temperature of LIBs. Wang et al. [63] studied the temperature distribution of large power batteries at different discharge rates and discharge depths through infrared thermal imaging technology. The experimental results showed that the direction of heat flow between the collector and the cell was different. In the discharge process, the high-temperature area was stable in the middle of the battery during low-rate discharge, and the high temperature was close to the positive terminal during high-rate discharge. The temperature variance (T^2_{var}) was proposed for the first time to express the temperature uniformity of the battery cell. T^2_{var} has a rapid change trend in the initial and final stages of high-power discharge, which represents the risk of TR.

$$T^2_{var} = \sum_i^n f_i (x_i - \overline{x})^2 \qquad (17)$$

where f_i denotes the frequency of a 0.1 °C temperature range, and $\overline{x}$ denotes the average of total temperature data.

However, the research of Sun et al. [64] showed that there was a certain difference between the surface temperature and the internal core temperature of the LIBs during operation. Parhizi et al. [65] used surface temperature and chemical kinetics data to determine the core temperature during the TR process. The research results showed that the core temperature was about 100 °C higher than the surface temperature during TR. The LIB is a completely closed space, and the surface temperature cannot fully reflect the internal state of the battery, so there is a certain temperature difference between the inside and outside of the battery and different positions. Therefore, only measuring the temperature at a certain point on the battery surface cannot accurately predict TR. Given this, the thermocouple based on the flexible ultra-thin structure (TFTC) was prepared and wrapped with polymer to avoid the corrosion of the electrolyte inside the battery, and then transferred to the copper foil collector of the battery for the in-situ internal temperature measurement [66,67]. Zhu et al. [68] integrated a multi-point film sensor into the battery electrode. The long-term cycle test and electrochemical impedance test showed that the integrated film sensor in the electrode had little impact on the cycle performance of the LIBs, and it could measure the multi-point temperature change in the battery at different magnifications in real time. Li et al. [69] successfully measured the internal temperature of LIBs with a resistive temperature detector (RTD). Furthermore, a direct electrode temperature measurement technique based on additive manufacturing enabled the application of additive manufacturing was proposed [70]. The initial temperature of the SEI film decomposition monitored by the built-in RTD was 10 s earlier than that of the battery surface sensor.
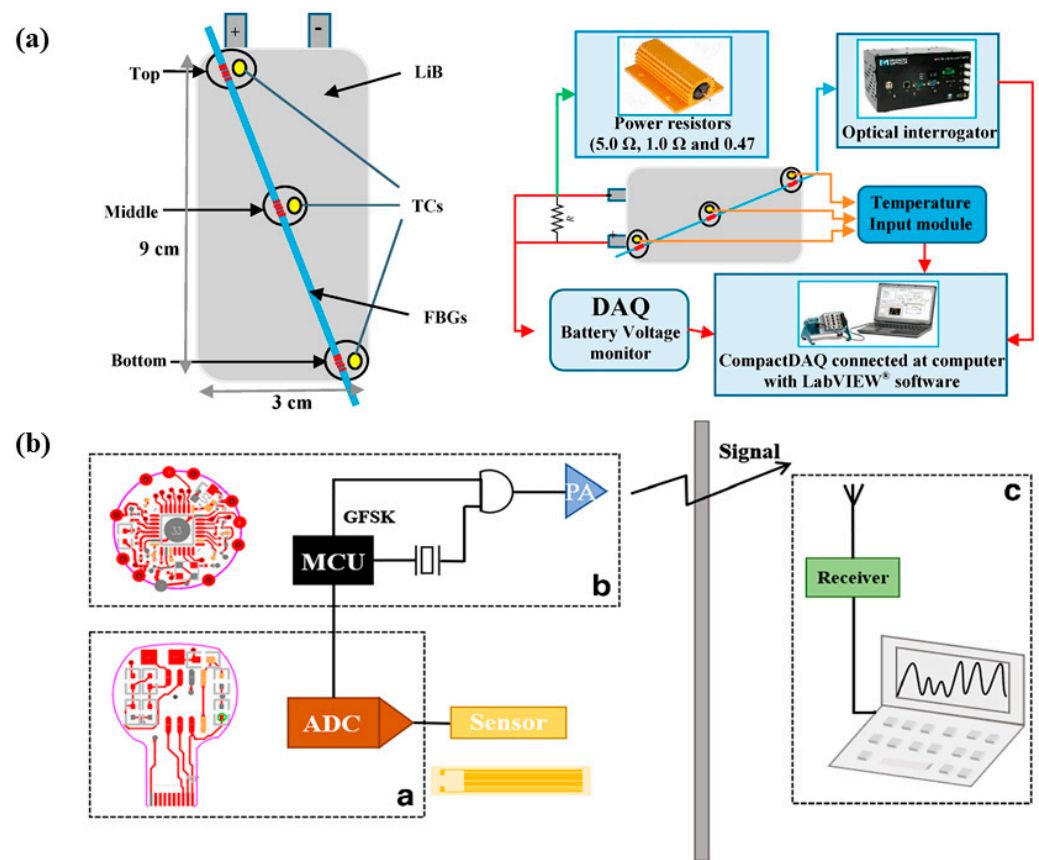
3.2.2. Optic Fiber Sensor

Optical fiber sensors are also widely used in the temperature measurement of LIBs. Light sensors are small in size and have good elasticity, insulation, corrosion resistance, and other properties; therefore, they can be used in the external and internal battery environment. As the internal reaction of the battery generates heat and the temperature rises, the optical signal transmitted by the optical fiber will change. Nascimento et al. [71,72] compared the sensitivity of fiber Bragg grating (FBG) and thermocouple in the cycle process at different magnifications, and monitored three positions at the top, middle, and bottom of the battery. The layout location and schematic diagram are shown in Figure 3a. The results show that the thermal response rate of FBG is 1.2 times faster than that of thermocouple, i.e., 4.88 and 4.10 °C/min respectively. Furthermore, through FBG, the thermal behavior of LIBs in different environments was monitored in real time, in situ, and operando [73].

At present, most LIBs use winding structures, and the response speed of external temperature and external rupture gas production is much lower than that of the battery interior. When TR is about to occur, the temperature sensors, pressure sensors, gas sensors, etc. on the battery shell cannot be obtained in a timely manner, and early warnings cannot be made. Therefore, the real-time transmission of the internal signals of LIBs is crucial. The internal temperature of the battery is the most direct method to reflect the internal state of the LIBs, which can effectively reflect the internal real-time state and achieve early warning of TR. Fleming et al. [74] fabricated a FBG sensor and built it into a commercial 18,650 battery. The results of Electrochemical Impedance Spectroscopy (EIS), Computed Tomography (CT) scan, and cycle test indicated that the sensor had little influence on the electrochemical performance of the battery. The results showed that the temperature difference between inside and outside the discharge stage was up to 6 °C. Accurate internal temperature monitoring of the battery is a very important technology for early warning of LIB TR. However, the position of the optical fiber sensor is easy to shift along with the usage of batteries, which will lead to inaccurate temperature measurement and battery performance degradation [75].

Traditional wired sensors break the sealing structure of LIBs. Although they are disassembled and installed in glove boxes or drying rooms with very low water and oxygen content, immature packaging technology inevitably affects battery performance.

The method of wireless data transmission is expected to solve the sealing problem of LIBs caused by traditional methods and establish a real-time monitoring method for the internal signals of batteries. Chen et al. [76] first applied implantable wireless signal transmission technology to internal battery monitoring. As shown in Figure 3b, by means of temperature sensing in part (a), data transmission in part (b), and data recovery in part (c), a real-time monitoring data sensing system is realized, which can accurately measure the internal temperature and send stable signals in real time under different power ratios, achieving a sampling frequency of 4 Hz and sampling accuracy of 0.05 °C.

In conclusion, due to the temperature gradient between the external temperature and the actual internal temperature of LIBs, the internal temperature monitoring of LIBs can perceive the internal temperature change information of the battery quickly and early so as to achieve the early detection of TR, leaving more time for the subsequent emergency disposal.

Figure 3. Thermal signal safety monitoring method. (**a**) Optical fiber sensor and thermocouple layout position (**right**) and schematic diagram (**left**) (use LabVIEW® customized application) [71]; (**b**) implantable wireless signal transmission technology [76].

3.3. Safety Warning Technology Based on Force Signal

The monitoring methods of battery TR based on force signals are mainly divided into two types. One is the internal stress of the battery. During the overcharge and over-discharge process of LIBs, Li$^+$ is constantly embedded/disembedded at the electrodes, resulting in structural changes of the active material, so the cell thickness will change slightly [77,78]. When the battery is abused, the internal heat of the battery continuously accumulates, and the temperature rises, which generates a large volume of gas products. The increase in the battery internal pressure also causes the stress change. At present, LIBs are mainly aluminum plastic film packaged flexible batteries and aluminum alloy prismatic batteries. Due to the good extensibility of aluminum plastic film packaging, it is greatly deformed when misused. However, most of the batteries used steel shell structures with

safety valves. Once the internal pressure of the battery accumulates more than the sum of the external pressure and the pressure relief valve stress, the safety valve opens. Therefore, the shock pressure caused by the gas ejected from the safety valve in the form of a shock wave during the battery TR can also be used as a safety warning, as shown in Figure 4 [79].
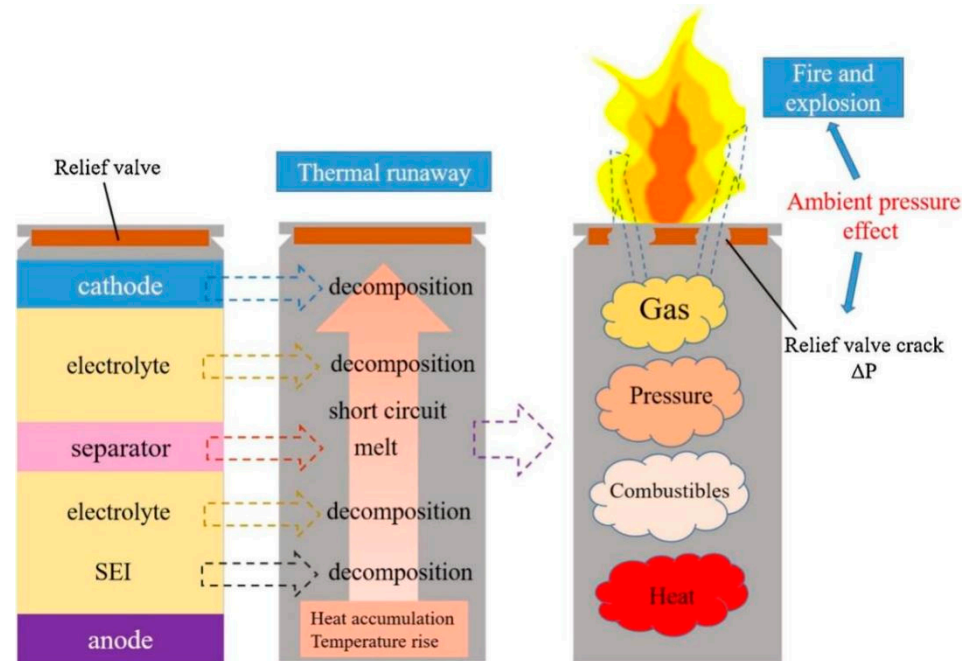
Figure 4. The shock pressure caused by the ejected gas [79].

### 3.3.1. Internal Stress of Battery

The expansion force of LIBs is affected by many factors, such as the type of cathode and anode active substances inside the battery, the SOC and SOH of the battery, and the external environment. When a battery is abused, the expansion of the battery due to gas production can also cause significant deformation of the battery casing. Therefore, by specifying the change range of normal and abnormal expansion force of LIBs and combining it with relevant sensors to detect the expansion force of the battery, an effective warning can be made about the occurrence of TR. Sommer et al. [80,81] measured battery strain during charging and discharging by connecting an external Fiber Bragg Grating optical fiber sensor. They found that the battery had volume deformation during charging and discharging. Zhang and Hahn et al. [82,83] analyzed the contribution of various components to the volume deformation in the charging and discharging of commercial LIBs, and concluded that the insertion and removal of lithium in the battery anode was the main reason for the volume deformation. The strain change is mainly affected by the deformation of the anode. Zhu et al. [84,85] measured the circular internal strain of 18,650 LIBs using a thin film strain sensor. The strain increases with the increase of the SOC during charging. The strain change is related to the lithium content between electrodes. The deformation and failure of anode materials play an important role in the internal short circuit and TR behavior of LIBs. Wang et al. [86] studied the strain effect of the battery anode. The results showed that when the LIBs were about to undergo TR, the expansion force of the cell changed significantly compared with normal charging and discharging. The early failure of anode materials under a high strain rate may be one of the main reasons for the early short circuits of the battery under dynamic impact. Therefore, monitoring the change in the expansion stress of LIBs is also a means of warning about TR. The batteries in a battery pack are closely arranged. If one of the batteries is deformed or expanded, the surrounding batteries will be squeezed and finally crack. Sun et al. [87] recorded the deformation in the overcharge process of the pouch cells, and established the expansion model of the battery

under overcharge abuse. After overcharge, the battery underwent obvious deformation, which significantly increased the squeezing force on batteries within a battery pack.

3.3.2. Shock Pressure

The gas generated by the battery TR causes shock-pressure harm in the form of a shock wave. In addition, LIBs are mostly arranged in enclosed or semi-enclosed spaces; their injection rapidly increases the pressure inside the space. Gas impact pressure measurement is a low-delay, low-cost, and reusable test method, and the sensor detecting pressure can be placed anywhere in the battery pack or module.

Wang et al. [48] studied the fire and explosion characteristics of the NCM811 battery TR in a confined space. The results showed that the environmental pressure had risen before the voltage drops and the temperature rises, which could be used as an early warning signal of battery TR in a confined space. Koch et al. [88] used a variety of sensors to simultaneously monitor the TR behavior of a battery, including pressure sensors. The test results showed that the pressure sensor could detect the TR about 5 s before the temperature sensor, as shown in Figure 5a. Chen et al. [89] studied the experimental device for the TR shock pressure of 18,650 batteries in a semi-enclosed space, as shown in Figure 5b. The results show that the over-pressure release was a strong shock process. Although the impact pressure range of the safety valve opening was small and short, the conventional pressure sensor could detect this signal, and further measures might be taken to prevent the battery from TR. The interval between the opening of the safety valve and the violent injection was approximately 384 s, which provided sufficient time for countermeasures. Moreover, the TR over-pressure would be more obvious in the severe injection phase.
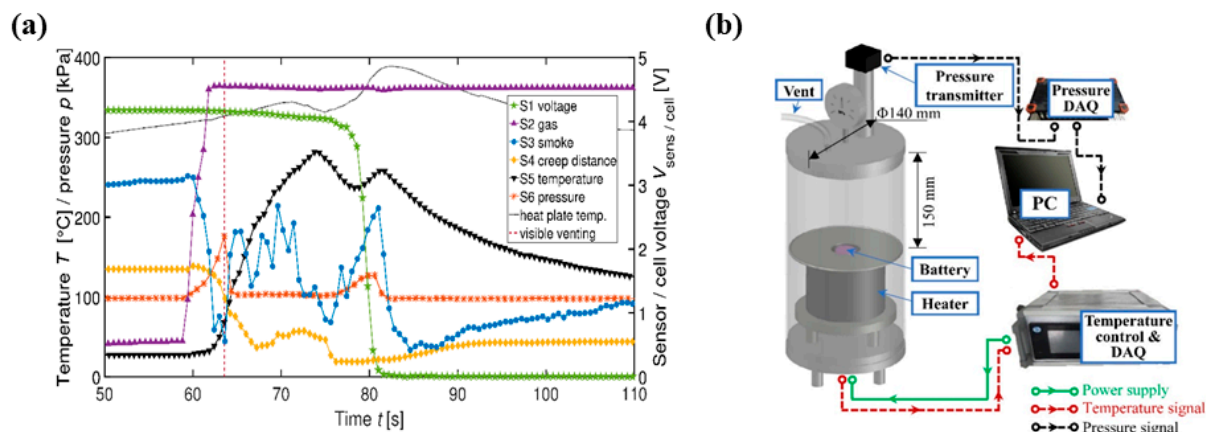
Figure 5. Through the shock pressure to detect TR: (**a**) multiple sensors detect TR of battery [88]; (**b**) experimental device for the TR shock pressure [89].

3.4. Safety Warning Technology Based on Electric Signal

3.4.1. Electrochemical Impedance Spectroscopy

EIS is a method used to analyze the physical and chemical processes of a battery, and the EIS test does not cause any damage to the battery. The electrode process within the battery is equivalent to a simple circuit composed of resistance and capacitance in series and parallel. The corresponding output signal can be obtained by inputting the disturbance signal through the electrochemical workstation. The measured EIS spectrum with the determined equivalent circuit or mathematical model can infer the dynamic process/mechanism contained in the battery and obtain more information on the electrode process/dynamics and electrode interphase structure. EIS can be used as an effective tool to monitor battery status, and these parameters can be used as indicators of early battery failure and early warnings. Impedance phase shift and amplitude can be used to monitor and predict the internal temperature of LIBs [90], as shown in Figure 6a. Liu et al. [91] characterized the electrochemical parameters of LFP batteries during cyclic overcharge. Compared with

voltage, capacity, and temperature, the impedance changed more significantly. The results showed that the increase of SEI/cathode electrolyte interphase (CEI) film resistance, charge transfer resistance, and Warburg coefficient were the main changes in the process of cyclic overcharge. Srinivasan et al. [92] confirmed that the phase shift of battery impedance was strongly related to temperature, which means that predicting battery temperature through electrochemical impedance has become a feasible means. Furthermore, Srinivasan [93] found that the phase shift of LIBs changed significantly before battery exhaust and TR. As shown in Figure 6b, with an increase in battery temperature, φ changes from a larger negative value to a smaller negative value. However, about one minute before the exhaust of the LIB, the φ value shows a significant change from −0.88 to −2.82, while the battery voltage and the battery surface temperature did not change significantly. By measuring the phase shift, the internal temperature of the battery could be quickly predicted, and the phase shift accuracy was convincing at a specific frequency; meanwhile, the requirements for the capacity size of LIBs were low.
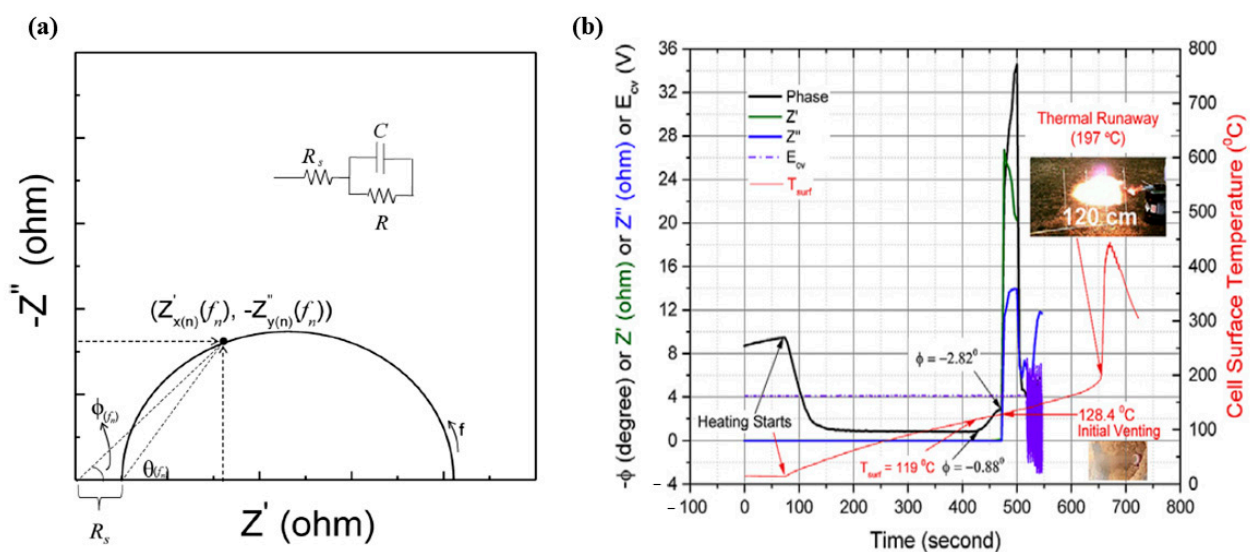
Figure 6. Through electrochemical impedance spectroscopy to detect TR: (**a**) Nyquist representation of the electrical impedance [90]; (**b**) Phase shift change before battery TR [93].

Compared with the above-mentioned technical methods for temperature monitoring, it is a reliable method for predicting the internal temperature of LIBs through the phase change and amplitude of electrochemical impedance. It does not need to invade the battery or use large temperature-measuring equipment.

On the other hand, impedance measurement at a specific frequency only warns about one stage of temperature, and its reliability is not high. Therefore, Dong et al. [94] developed a method of two stages and three indicators, aiming at the two stages of abnormal temperature rise inside the battery and before a sudden temperature rise. As shown in Figure 7, three indicators are proposed for the convergence of phase angle at an intermediate frequency, the confusion of impedance curve at high frequency, and the deviation of impedance point at low frequency. According to the accelerating rate calorimetry (ARC) experiment, the three indicators proposed can give an early warning before the battery self-heating onset and TR trigger. The implementation of multi-stage and multi-index hierarchical early warnings for batteries makes the early warning time advance and the reliability greatly improve.
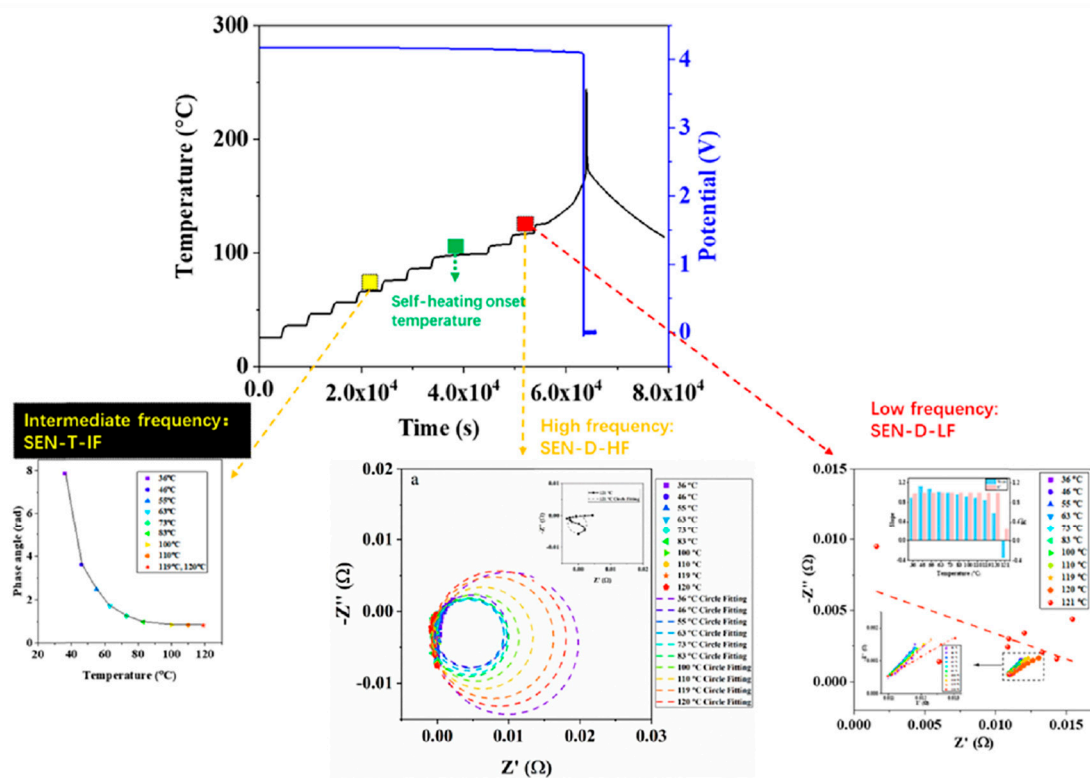
Figure 7. The EIS-derived indicators in the intermediate-frequency, low-frequency, and high-frequency are used to give reliable and early warnings of TR [94].

Predicting the internal temperature state of LIBs through the phase shift, amplitude, real part, and imaginary part of electrochemical impedance often requires data modification, and depends on complex mathematical models, which are not suitable for predicting the battery TR. In addition, EIS measurement takes a long time, which seriously hinders the prediction of TR. Lyu et al. [95] found that when a 48 Ah LFP battery was overcharged at the beginning, the real-time dynamic impedance had a slope from negative to positive at 30–90 Hz, as shown in Figure 8a. A dynamic impedance measuring device was further designed. By monitoring the 70 Hz dynamic impedance, an early warning could be given 580 s before the occurrence of TR. As shown in Figure 8b, the inflection point of impedance was more obvious and closer to the beginning of overcharging than the voltage and battery surface temperature.

3.4.2. Internal Short Circuit

The battery TR under different abusive modes has a common internal short circuit (ISC) [96]. When the separator melts, the voltage drops slightly. For many steel-shell LIBs with safety valves, when the internal pressure reaches a certain level, the safety valve opens, and the voltage drops suddenly. Therefore, another early warning method for battery TR is terminal voltage.

The root cause of many LIB accidents is that one of the batteries had an ISC, which causes the TR to spread among the batteries even in the battery pack. Therefore, the ISC of LIBs is an early sign of impending TR. The research of Zhong et al. [97] showed that the time difference between voltage drop and TR of 18,650 ternary LIBs was 127–409 s. This also verified the importance of ISC for TR warning of LIBs and implied that ISC could be used as an early parameter for TR warning of LIBs. Feng et al. [98,99] proposed an online detection algorithm for the ISC of large LIBs, which detected early ISC based on voltage and temperature response through the 3D electrical thermal ISC coupled model, and did not need to consider the location of ISC inside the battery. This algorithm could give an early warning more than 30 min before the occurrence of TR. In addition, they [100] put forward

a TR detection method based on battery consistency in the battery pack. This method uses the recursive least square TR algorithm based on the mean difference model (MDM). In the case of ISC, the characteristic parameters such as voltage difference and internal resistance fluctuation function would change significantly. Sazhin et al. [101] proposed a method for battery ISC detection and safety assessment, which was determined by the self-discharge current under potentiostatic conditions at a slight discharge over-voltage. By balancing the battery with the direct current (DC) voltage source, the DC applied a voltage slightly lower than the battery open-circuit voltage (OCV) or initial voltage, generating current in the circuit in response to potentiostatic polarization. Determine whether ISC occurs by judging the change of current direction between the tested battery and the DC voltage source.
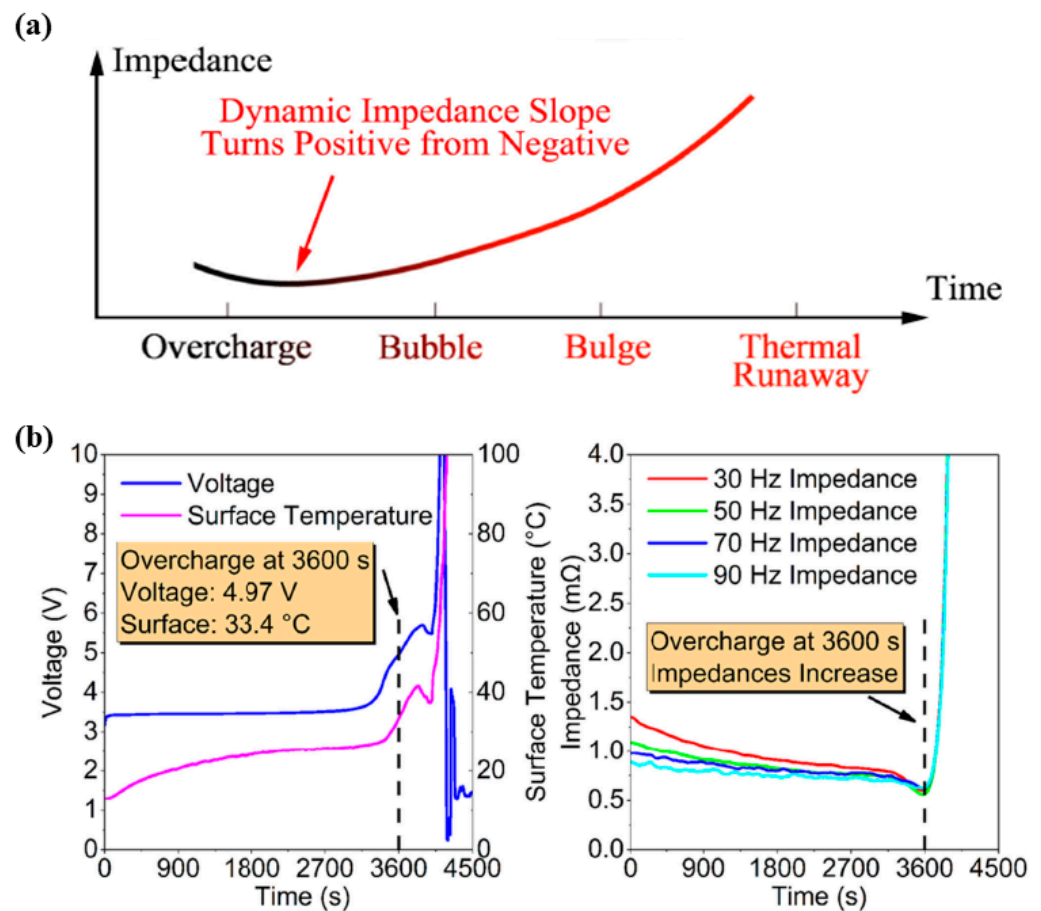
Figure 8. Through the real-time dynamic impedance to detect TR: (**a**) real-time dynamic impedance slope change during battery overcharge [95]; (**b**) the inflection points of impedance, voltage, and temperature [95].

3.5. Safety Warning Technology Based on Gas Signal

The side reactions between electrolyte and electrode cause a large amount of gas to be generated inside the battery, along with TR. When the gas volume accumulates to a certain extent, it is released. At present, the monitoring methods for LIB gas production mainly focus on the use of mass spectrometry-spectral sensors, traditional gas sensors, and optical fiber sensors.

3.5.1. Mass Spectrometry and Spectral Sensors

It is a feasible monitoring method to identify the gas released from LIBs by mass spectrometry and spectral sensors. GC-MS technology refers to the combination of a gas chromatograph and mass spectrometer for material analysis. Fernandes et al. [102] used GC-MS to identify and quantify the gas production of 2.5 Ah and 26,650 LFP LIBs in the

process of overcharge abuse. The results showed that in the early stage of battery TR, solvent vapor was first released. When the metal shell cracked, the gas production rate and concentration rose sharply. Although GC-MS has high sensitivity, the gas within the battery must be connected to the sampling port when using GC-MS to measure the gas produced by LIBs, and the gas must be extracted from the battery. FTIR technology refers to converting the original interferogram into the actual spectrum through Fourier transform. In the range of 600–4000 cm^{-1}, the material composition is determined by the main specific molecular groups in the sample. Essl et al. [103] used an FTIR spectrometer to quantify the TR gas production of NMC LIBs online, and proposed a measurement method with hydrogen fluoride (HF). Larsson et al. [104] used the single burning item (SBI) test method and online FTIR to quantitatively study the fluoride gas release of seven types of LIBs when they were on fire. A large amount of HF was detected in the experiment. For batteries with nominal capacity (Wh), the amount of HF produced can reach 20–200 mg/Wh, which may pose a serious toxic hazard to human beings. Toxic and flammable gases can be used as key parameters for early failure monitoring of LIB TR. Raman spectroscopy is a kind of scattering spectrum. It is an analytical method to analyze the scattering spectrum different from the incident light frequency to obtain the information of molecular vibration and rotation, and it can be applied to research on the molecular structure. Od-Gerelt et al. [105] designed a device to collect gas from 18,650 batteries by Raman spectroscopy. H_2, methane, CO_2 and CO were the main detected gases. At first, the changes in CO and CO_2 were significant, but with the increase of cut-off potentials, the contents of H_2 (4.2–4.4 V) and methane (>4.6 V) suddenly increased. Liao et al. [106] built an early warning device for battery TR using a cantilever-enhanced photoacoustic spectrometer (CEPAS). The infrared beam was processed by an optical filter and a mechanical filter to form a narrowband infrared beam, which was emitted into the photoacoustic cell. At the same time, the characteristic gas discharged from the LIBs entered the photoacoustic pool through the particle filter and absorbed the energy of the narrow-band infrared beam to produce periodic vibration and the photoacoustic effect, which made the cantilever deform and obtained the corresponding voltage signal. The warning system is shown in Figure 9.
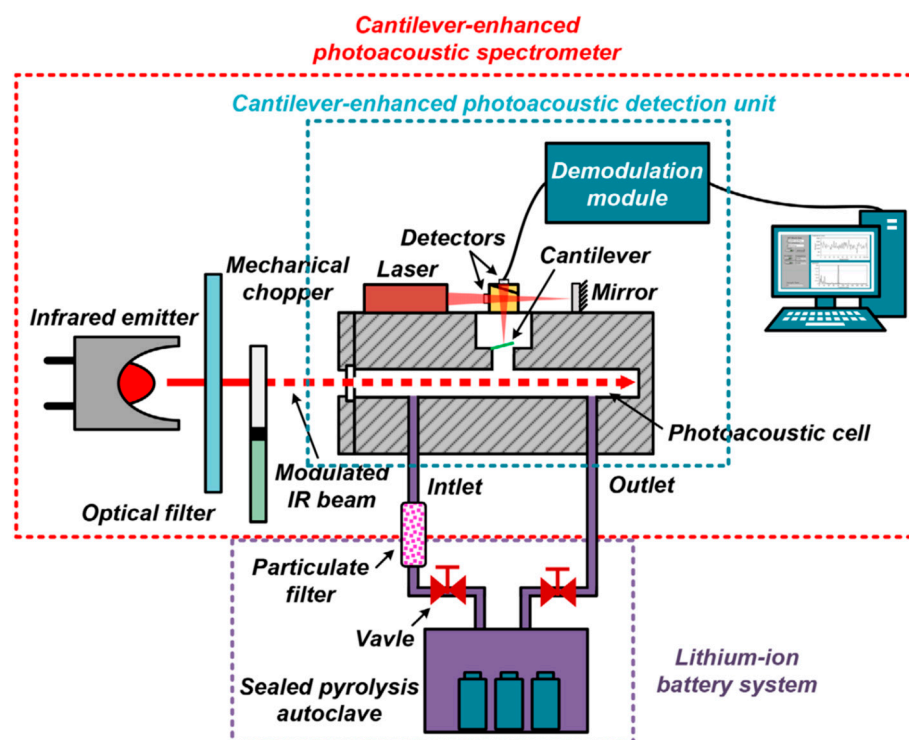

Figure 9. Cantilever-enhanced photoacoustic spectrometer battery TR warning system [106].

3.5.2. Gas Sensor

After the safety valve is opened, LIBs produce a large amount of gas, with a fast gas flow rate and large gas production. The gas sensor can effectively monitor battery TR gas production, and it is also a widely used TR warning method. Yuan et al. [107,108] found that NCA and LFP LIBs released a large number of highly flammable hydrogen and hydrocarbons due to TR. Among these gases, H_2 and CO accounted for the largest proportion, which could be used as the characteristic gases of LIBs. When the LIBs were overcharged, the metal Li reacted with polymer binders to produce a certain amount of H_2. Given this, Jin et al. [109] developed a sensitive TR monitoring and warning method based on capturing H_2, which could detect the formation of lithium dendrites in the micron scale (~50 μm) on the anode. As shown in Figure 10, through the verification of LFP battery overcharge, the results showed that lithium dendrites grew continuously at the anode during overcharge and reacted with PVDF binder to produce H_2, which was released through the safety valve and captured 435 s before smoke and 580 s before ignition. Early detection of battery TR provides more valuable time for accident countermeasures. Therefore, it is an effective means to monitor the early warning of battery TR by configuring gas sensors near the battery pack.
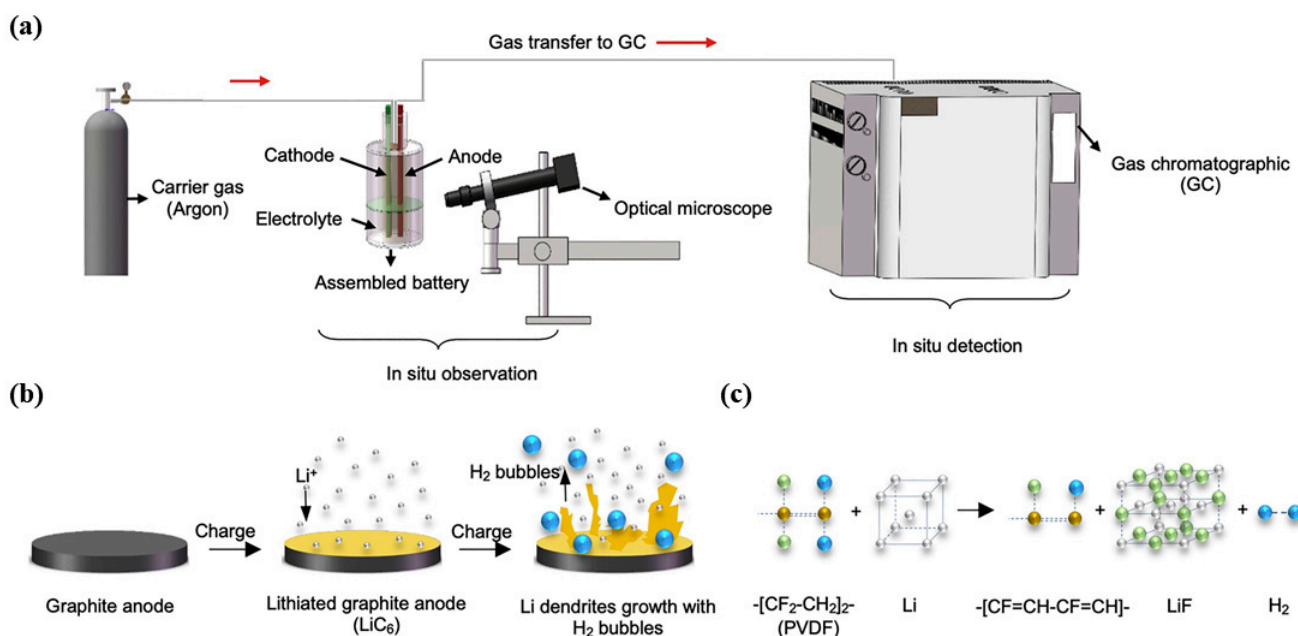
Figure 10. Sensitive TR monitoring and warning system based on capturing H_2 [109]: (**a**) Li dendrite growth observation and H_2 capture system, (**b**) H_2 generation mechanism and (**c**) Reaction mechanism of Li dendrites and PVDF binder.

3.5.3. Optical Fiber Sensor

In the early stage of TR, the electrode and electrolyte inside the LIBs continue to decompose, and a certain amount of gas is generated inside the battery. Currently, the main method of gas monitoring for LIBs mainly relies on GC-MS (offline), which cannot monitor gas production while the battery is working. For FTIR that can be monitored online in real time, it is usually necessary to make special modifications to the battery, which is only applicable to specially designed testing batteries. Therefore, these two test methods cannot be used in actual commercial batteries. Optic fiber sensors, due to their compact shape, immunity to electromagnetic interference, and electrostatic discharge, offer the possibility of implantation into commercial batteries and early warning of battery TR.

The optical characteristics of the optical fiber sensor change with the concentration of the detected chemical substance. Lochbaum et al. [110] studied the evolution of CO_2 gas in LIBs under micro overcharge by embedding an optical fiber sensor in the battery, providing

a dynamic signal of gas evolution during overcharge. The experimental results showed that the gas generated in the battery during the overcharge cycle could not be reversed and that the internal sensing signal increased with each overcharge cycle.

3.6. Comparison of Typical Early Warning Methods

The advantages and disadvantages of typical monitoring and warning methods for TR have been compared and analyzed, as shown in Table 3. At present, the monitoring and warning methods based on acoustic signals are less studied and are vulnerable to the impact of the external environment with low accuracy. The monitoring and warning method based on thermal signal is intuitive and reliable and is widely used. The TR warning of the battery through stress monitoring is still in the research stage, and the monitoring is mostly aimed at a single battery, which cannot achieve large-scale warning, and the change of battery expansion is greatly affected by the battery status. The monitoring method based on electrical signal can monitor the battery status in real time, but the prediction accuracy is low, and the instrument is precise. The monitoring method based on a gas sensor can provide an accurate warning, but the gas concentration should be considered, and the remaining disposal time is relatively short. The built-in optical fiber sensor method can be used to measure information about the internal state of the battery in real time. Through the built-in sensors, the internal temperature, pressure, and gas signals of the battery can be obtained, and the battery management system can provide better intelligent management and early warning of TR. However, the geometric structure and internal space limitation of the battery must be considered for the internal sensor because once the sensor contacts the jelly roll, the position impedance may be increased, and the electrochemical performance of the battery will be greatly reduced. Therefore, the built-in sensor also needs to start with the manufacturer's production process. In addition, it is also necessary to optimize the sensor for the strong corrosive environment inside the battery so that it can have long-term operation inside the battery.

Table 3. Typical monitoring and warning methods for TR and their advantages and disadvantages.

Category	Specific Monitoring Method	Early Warning Parameter	Early Warning Time	Advantages	Disadvantages
Acoustic	Ultrasonic testing	TOF, amplitude	Warning before failure about 90 min [57]	Small size, easy to integrate in battery management system	Most of the research is focused on single battery and has not been studied on a large scale
	Acoustical signal	Safety valve opening sound	Venting acoustic signal is 618 s and 1061 s earlier than the fume and the fire, respectively [32]	Low price, no need to invade the battery	Low accuracy, easy to be affected by noise interference
Heat	Infrared	Distribution of temperature	/	Precise positioning, high accuracy	Only high temperature can be identified, unable to early warning
	Optic fiber sensors	Correspondence between optical fiber refraction wave and temperature change	/	Early warning, high accuracy	Destroy battery structure and reduce battery performance, high cost, complex process
	Thermocouple	Temperature	/	Low cost, easy installation	Low accuracy, unable to early warning
Force	Internal strain	Battery thickness change	/	High accuracy, fast detection	The change of Strain is not significant, and it is mostly for single battery
	Shock pressure	Gas shock pressure	Gas shock pressure is early than the TR approximately 384 s [89]	Low latency, low cost, significant changes	Unable to early warning

Table 3. *Cont.*

Category	Specific Monitoring Method	Early Warning Parameter	Early Warning Time	Advantages	Disadvantages
Electricity	Electrochemical impedance spectroscopy	Phase shift, amplitude	Warning time is 580 s ahead of the TR [95]	No need to invade the battery, early prediction	Unable to large-scale early warning, electrochemical measuring instrument precision, high price
	Internal short-circuit	Voltage and current change	ISC is observed to happen 300 s before TR [35]	Convenient for real-time monitoring, accurate positioning	Low prediction accuracy, complex sensors, and algorithms
Gas	Mass spectrometry and spectral sensors	Internal gas of the battery	/	High accuracy	Need to intrude into the battery and destroy the gas balance in the battery, instrument precision
	gas sensor	Gas and electrolyte vapor generated after battery TR	Gas capture time is 639 s earlier than smoke and 769 s earlier than fire [109]	Unable to early warning, leaving short time for later prevention and control, reliable and stable	The gas needs to reach a certain concentration before it can be detected, and the TR position cannot be accurately located
	Optic fiber sensors	Corresponding relationship between gas concentration and optical fiber	/	High accuracy	Destroy battery structure and reduce battery performance, high cost, complex process

4. Fire Extinguishing Technology of Lithium-Ion Batteries

The ignition of LIBs requires some critical conditions (i.e., combustible, oxidant, and ignition source). Combustibles refer to the flammable substances of the LIBs themselves and the flammable substances produced by them. The oxidant comes from the oxygen generated by the decomposition of the battery at a high temperature and the oxygen contained in the air. The ignition source mainly refers to the heat generated by the internal reaction of the battery and the external heat source [111]. Passive protection of LIBs is the last barrier preventing the deterioration of battery TR. The effect of firefighting determines the severity of LIB fire accidents. Therefore, the selection of fire extinguishing agents has become another focus of battery TR prevention and control. At present, the commonly used fire extinguishing agents for LIBs are mainly divided into solid fire extinguishing agents, gas fire extinguishing agents, and liquid fire extinguishing agents according to the phase classification. The advantages and disadvantages of these three types of fire extinguishing agents for battery fire are summarized as well.

4.1. Gas Fire Extinguishing Agent

Gas fire extinguishing agents have the advantages of no residue, environmental friendliness, and no damage to equipment. At present, the gas fire extinguishing agents for battery fires mainly include halon, carbon dioxide, heptafluoropropane, dodeca-fluoro-2-methylpentan-3-one, and 2-BTP new gas fire extinguishing agents.

The Federal Aviation Administration (FAA) [112] reported the inhibition effect of halon series (Halon 1301, 1211, etc.) fire extinguishing agents on battery TR. Halon fire extinguishing agents can effectively inhibit the combustion of LIBs, but the batteries are prone to reigniting after firefighting, and halon's ozone consumption capacity is extremely high, which is a culprit of global warming. Therefore, halon fire extinguishing agents have been banned worldwide since 2010.

With carbon dioxide, the extinguishing mechanism is asphyxiation and cooling. When the carbon dioxide extinguishing agent is released, the oxygen concentration rapidly decreases, and the flame is extinguished. At the same time, carbon dioxide, as an inert gas

extinguishing agent, also plays a role in explosion suppression. However, the battery TR is a process in which oxygen will be spontaneously generated inside the battery. Therefore, it is difficult for carbon dioxide to completely inhibit the TR reaction of the battery. Once the battery in TR contacts with fresh air, it is likely to be reignited. Si et al. [113] injected CO_2 at 0.5 Mpa injection pressure when there was an open flame in the battery. Although the flame did not burn continuously, the temperature of the battery still rose during the CO_2 injection process, which indicated that the heat generation rate of LIB combustion was still greater than the cooling rate of CO_2.

The fire extinguishing mechanism of heptafluoropropane (HFC-227ea) is mainly physical cooling and chemical inhibition [114]. Physical cooling mainly refers to the heat absorbed from the flame during the conversion of the liquid HFC-227ea extinguishing agent into gas, and the energy absorbed through the fluorine bond that destroys good stability when decomposing HFC-227ea vapor. Chemical inhibition forms fluorocarbon compounds through the thermal decomposition of HFC-227ea, consumes O, H, and OH free radicals in the combustion chain, and interrupts the chain reaction [115]. The detailed mechanism is shown in Figure 11a. Liu et al. [116] showed that HFC-227ea could quickly extinguish the open flame of the battery, and its inhibition effect on temperature rise was obviously superior to ABC dry powder and CO_2. Si et al. [113] sprayed HFC-227ea immediately after the battery caught fire. It was found that reducing the spray flow and prolonging the spray time could improve the fire extinguishing effect without generating a continuous flame. Rao et al. [117] compared the fire extinguishing effects of HFC-227ea and CO_2 fire extinguishing agents on LFP batteries used on ships. The results showed that HFC-227ea was more effective on battery fires than CO_2. Zhang et al. [118] found that although HFC-227ea effectively reduced the fire power, it was still difficult to put out a 243 Ah large LFP battery fire.

As a new substitute for halon, dodecafluoro-2-methylpentan-3-one (Novec-1230) has good insulation, chemical inhibition, and environmental protection performance, and has the potential ability to extinguish LIB fire. Its fire extinguishing mechanism mainly involves physical cooling and blocking chemical combustion reactions to convert H and OH free radicals into stable HF and CF_2O. Its inhibition mechanism is shown in Figure 11b [119]. Wang et al. [120] built a Novec-1230 fire extinguishing experimental system and simulated a real fire situation in the actual application of batteries. Based on the NFPA2001 standard for clean agent fire extinguishing systems and Equations (18) and (19), the required concentration of Novec-1230 extinguishant was calculated. Their results showed that Novec-1230 could effectively extinguish battery fires in both open and confined spaces, and the fire extinguishing efficiency of Novec-1230 was much higher than that of the CO_2 extinguishant.

$$W = \frac{V}{S}\left(\frac{C}{100 - C}\right) \tag{18}$$

$$S = 0.000275T + 0.066054 \tag{19}$$

where w is the weight of the clean agent, V is the net volume of hazard, S is the specific volume of the superheated agent vapor in the standard atmosphere, C is the agent design concentration, and T is the minimum anticipated temperature of the protected volume.

Further, Liu et al. [121] found that the relationship between the inhibitory effect and dose of Novec-1230 has a critical value (X_{inc}), which gradually transformed into an inhibitory effect when the dose is increased beyond the X_{inc}. The cooling rate of the Novec-1230 fire extinguishing agent is not obviously compared with the heating rate of the battery, and other auxiliary means such as coordinated cooling of liquid extinguishing agent are needed. The battery TR will bring great fire and continuous thermal hazards. Considering that Novec-1230 can effectively inhibit LIB fire, but its cooling effect on LIBs is not obvious, it may be an efficient method to cooperate with Novec-1230 to extinguish fire by cooling with a water-based fire extinguishing agent. A new safety strategy for LIBs integrating fire extinguishing and rapid cooling was proposed [122]. By combining Novec-1230 with water

mist, Novec-1230 was sprayed to extinguish the fire when TR occurs, and then the battery was cooled by water mist. The peak temperature and high temperature duration of the LIBs were significantly reduced. Further, Liu et al. [123] studied the inhibition and toxicity of various inhibitor doses of Novec-1230 on a 300 Ah LFP battery fire. The results showed that high inhibitor doses of Novec-1230 increased the toxicity of the system, with the main toxic gas of CO and irritating gases of HCl, NO_X and HF.

Figure 11. Fire extinguishing mechanism of (**a**) HFC-227ea [115] and (**b**) Novec-1230 [122].

2-BTP (2-bromo-3,3,3-trifluoropropene), as a new clean gas fire extinguishing agent instead of halon, has gradually been applied to extinguish battery fires. The mechanism is mainly that 2-BTP decomposes free radicals Br and CF_3 at high temperatures, which combine with H, OH, and O in the battery flame, greatly reducing the concentration of free radicals [124]. Xu et al. [125] studied the fire extinguishing effect of 2-BTP on 75Ah battery fire, and compared it with water, HFC-227ea, and pentafluoroethane (HFC-125). The fire extinguishing time of 2-BTP was only 13 s, and no reignition occurred. Furthermore, Shen et al. [126] found that, compared with Novec-1230 and water mist, 2-BTP effectively reduced the CO concentration when the battery is TR. The research of He et al. [127] showed that 2-BTP was significantly better than Novec-1230 in cooling and inhibiting temperature rise under low-voltage situations and can better inhibited runaway heat transmission between batteries.

Aerosol particles can be as small as micrometers, with strong diffusivity, which can avoid obstacles and flow, and can drill into tiny voids. Its properties are similar to those of gas, and it is a solid particle with a large surface area. The heterogeneous recombination of the free radicals in the flame chain propagation on the surface of the aerosol extinguishant is increased, the fire extinguishing efficiency is higher, and the initial cost and service life cost are relatively low. Robert et al. [128] tested the applicability of the aerosol fire extinguishing agent to a battery fire and used aerosol to extinguish a 1.9 kWh battery stored in a 40 foot container. The experimental results showed that aerosol at a density of 61 g/m^3 inhibited the battery fire, and the battery did not reignite within 30 min. Det Norske Veritas (DNV) [129] extinguished the battery fire through aerosol. The results showed that the aerosol could extinguish the fire in a relatively closed space, greatly reducing the oxygen content in the confined space. However, if oxygen reenters the battery system, it may lead to fire recurrence. Considering that the aerosol is difficult to volatilize automatically, and the metal oxides in the particles are easy to cause short circuit of electrical equipment, which will affect the visibility, reduce the oxygen concentration, and is not conducive to the observation of fire by firefighters. Therefore, aerosol fire extinguishing agents might not be suitable for suppressing the combustion and explosion of batteries.

However, some gas fire extinguishing agents are asphyxiating and toxic, which have serious harm to human life, and the cooling efficiency of gas fire extinguishing agents is not competitive compared with other types of fire extinguishing agent. It can be properly selected and applied in combination with the liquid extinguishing agent with a high cooling rate. The new clean gas extinguishing agent should be studied deeply, and the battery gas extinguishing agent should be comprehensively evaluated.
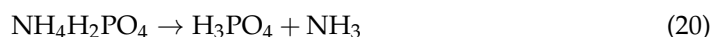
4.2. Solid Extinguishing Agent

Solid fire extinguishing agents are widely used, mainly including dry powder fire extinguishing agents, as well as dry water fire extinguishing agent of new solid powder. The fire extinguishing mechanism and application of a solid fire extinguishing agent in battery fire will be discussed below.

4.2.1. Dry Powder Extinguishing Agent

Dry powder extinguishing agents have the advantages of low toxicity, wide sources, and low cost. They contain BC dry powder, ABC dry powder, and D dry powder according to the fire type. BC dry powder is mainly sodium bicarbonate, which is used to extinguish Class B flammable liquid fire and Class C gas fire. ABC dry powder is made of ammonium dihydrogen phosphate, which can extinguish Class A solid material fire, Class B liquid fire, and Class C gas fire. D dry powder fire extinguishing agent is mainly composed of sodium chloride, which is used to extinguish combustible metal fires. At present, BC dry powder and ABC dry powder are mainly used in battery fire, and their fire extinguishing mechanisms mainly consist of physical and chemical aspects. Physical mechanism mainly refers to isolation, cooling, and asphyxiation. It forms an isolation layer by covering the solid powder on the surface of the combustibles, thus weakening flame combustion. In addition, the release of water vapor when the powder encounters high temperatures after being ejected and the decomposition reaction absorbing heat can achieve the cooling target. The inert gas generated by the decomposition of dry powder can dilute the oxygen concentration around the flame, thus playing the role of asphyxiation. Its chemical inhibition mechanism is to consume OH and H free radicals during combustion.

Reif et al. [130] suggested that water should not be used to extinguish the battery fire since the reaction between water and lithium metal would generate flammable and explosive H_2, instead they recommended using a dry powder extinguishing agent to extinguish the fire. In addition, the cooling methods for water and dry powder are different. Since the boiling temperature of water is 100 °C, the high temperature water evaporates rapidly, while the dry powder settles and covers the battery surface after spraying, which can cool the battery for a long time, but its cooling efficiency is not as good as water. Zhao et al. [131] compared the extinguishing effect of BC dry powder and ABC dry powder on 18,650 LIB fire, and the results showed that the cooling effect of ABC dry powder was better than that of BC dry powder. Meng et al. [132] discussed the extinguishing and cooling effect of ABC dry powder on LFP battery fire under different spraying distances, spraying angles, and spraying times. The experimental results showed that when the ammonium phosphate in the dry powder contacts the flame, the decomposition products volatilized at high temperatures to inhibit combustion and absorb a certain amount of heat. The endothermic decomposition reaction of ammonium dihydrogen phosphate under high temperatures is shown in Equations (20)–(23) [133].

$$NH_4H_2PO_4 \rightarrow H_3PO_4 + NH_3 \tag{20}$$

$$H_3PO_4 \rightarrow H_4P_2O_7 + H_2O \tag{21}$$

$$H_4P_2O_7 \rightarrow HPO_3 + H_2O \tag{22}$$

$$HPO_3 \rightarrow P_2O_5 + H_2O \tag{23}$$

4.2.2. Dry Water Extinguishing Agent

Dry water fire extinguishing agent is a new white powder fire extinguishing agent with distilled water as the main component inside and hydrophobic silica as the uniform coating on the outer surface [134]. The apparent property of the dry water extinguishing agent is similar to that of the dry powder extinguishing agent, which combines the advantages of traditional dry powder extinguishing agent and water mist extinguishing agent [135]. Compared with the dry powder extinguishing agent, the fire extinguishing time of the dry water fire extinguishing agent is shorter, and the cooling effect is better, but the residence time in the air is not long enough. Kong [136] prepared a dry water extinguishing agent containing additives. Their experimental results showed that the ammonium dihydrogen phosphate gel dry water extinguishing agent had the best cooling effect on the ternary LIB fire. Compared with the ABC dry powder extinguishing agent, the cooling effect of the ammonium dihydrogen phosphate gel dry water extinguishing agent was obviously better. Wang [137] carried out an experiment on the suppression of battery TR by dry water, which effectively suppressed and weakened the flame of battery TR and successfully interrupted TR propagation. After being driven by the explosion of the dry water extinguishing agent, the cladding structure is damaged such that the water phase and powder together quickly impact the fire source. To conclude, the dry water extinguishing agent is a promising, high-efficiency extinguishing agent for LIBs.

4.3. Liquid Extinguishing Agent

Liquid extinguishing agents mainly include water, water mist, water-based extinguishing agent with additives, hydrogel extinguishing agent, foam extinguishing agent, liquid nitrogen, vermiculite water dispersion extinguishing agent, etc. The application of liquid fire extinguishing agents in LIB fires and their extinguishing mechanisms are discussed in detail below.

4.3.1. Water-Based Extinguishing Agent

The cooling capacity of water is the strongest among many fire extinguishing agents with a maximum specific heat capacity of 4200 J/(kg·°C), and it is also the most widely used battery fire extinguishing agent at present. It has great advantages in extinguishing open flames and reducing the temperature of batteries.

Traditional water mist fire extinguishing technology has been proven to have a good fire extinguishing effect on battery fires and has been widely studied, but the water mist fire extinguishing technology is still not widely applied [138]. Liu [139] studied the TR suppression of 18,650 batteries with different SOCs by water mist through experiments. Their results showed that applying water mist before the critical temperature could prevent TR. The research of Larsson et al. [44] showed that in the process of water mist inhibiting the battery TR, the generation of HF could be affected. The release of water mist temporarily increases HF emissions, which might cause serious harm to firefighters. Wang et al. [140] summarized four fire extinguishing mechanisms of water mist. The primary fire extinguishing mechanism included heat absorption and cooling, mainly aimed at cooling the flame, wetting the surface of burning objects and forming a barrier to isolate external oxygen. The secondary extinguishing mechanism was the thermal radiation barrier and dynamic disturbance of the flame. However, the water mist of pure water without additives only plays a role in physical fire extinguishing; thus, the fire extinguishing efficiency is somewhat low [141]. Additionally, water is a conductive medium, which may cause partial or overall short circuit of the battery, further leading to battery failure when a large amount of water or water mist is sprayed. Adding a certain amount of additives in pure water can effectively extinguish the fire without short-circuiting the battery. Moreover, the additives can also reduce the water consumption required to extinguish LIB fire [142].

Cao et al. [143] found that adding 5% alkali metal salts (such as NaCl, KCl, and K_2CO_3) to ultrapure water mist could effectively enhance the explosion suppression effect. The type and concentration of additives had significant effects on flame propagation characteristics and explosion intensity. Zhou et al. [141] studied the inhibiting effect of low conductivity water mist containing additives on the battery TR, and determined the best components of fire extinguishing agent additives: 0.17% FC-4430 + 0.2% TEOA + 0.32% urea + 2.5% KCl. The experimental results showed that the synergistic action of physical and chemical additives significantly improved the fire extinguishing ability of fine water mist. Based on the above research results, Zhou et al. [144] further studied the water mist fire extinguishing agent for LIBs, and obtained the best components of 0.36% urea + 2.5% AEO-9 + 0.25% FC-4430 + 3.5% DMMP. Its cooling rate was 2.3 times that of water. AEO-9 had a remarkable synergistic effect, neutralized the electric repulsive force of other molecular (ionic) head groups in the surfactant, and formed a denser monolayer on the gas-liquid surface. Through the synergistic action between surfactants, the surface tension of water and the average particle size of water mist were effectively reduced. Through the synergistic mechanism of physical cooling of water mist and chemical inhibition of chemical additives, water mist with composite additives could well inhibit the intensity of battery fire and TR propagation.

In addition, the American Hazard Control Technologies, Inc. developed a new efficient, explosion-proof, and environment-friendly F-500 microcapsule fire extinguishing technology, which was widely used in fields such as building, fuel, coal, and metal fires. German motor vehicle inspection association (DEKRA) [142] compared the fire extinguishing effects of F-500, water, and dry powder extinguishant on LIB fires. The experimental results showed that the addition of F-500 could significantly improve the fire extinguishing efficiency of LIB fires, and the water consumption required for fire extinguishing was greatly reduced with a 1% F-500 extinguishant. Luo et al. [145] studied the fire extinguishing effect of 5% F-500 on LIBs. The F-500 solution quickly adsorbed and wrapped hydrocarbon molecules to isolate them from oxygen. Yuan et al. [107] selected a 3% F-500 solution to extinguish the battery fire. The gas adsorption experiment showed that the micelle size increased after 3% F-500 solution absorbed gas, indicating that it could adsorb explosive gases, such as H_2 and CO, generated by battery TR. By reducing the surface tension of water, F-500 improved the wettability of water and enhanced the possibility of water infiltration into the LIB gap. An enclosure was formed and maintained to make flammable hydrocarbons lose their combustibility and reduce the probability of reburning. Finally, the fire was extinguished quickly by blocking the free radicals of the chain reaction, and its extinguishing mechanism is shown in Figure 12.

The water mist has a certain effect on LIB fires, but the uniformity of the water mist and whether it can reach the combustion surface through the smoke generated by the battery should be considered. Water mist-containing additives have been widely studied, and the fire extinguishing efficiency has been significantly improved after adding additives. However, whether the conductivity of the extinguishing agent with additives will cause short circuit and other effects on the battery should be noted.

4.3.2. Hydrogel Extinguishing Agent

As a traditional fire extinguishing agent, water cannot effectively adhere to the surface of combustible materials, so the flame is prone to re-ignition. Thermosensitive hydrogels are widely used in fire protection. Under the influence of the external temperature, the phase change from sol to gel will be realized. When the temperature is lower than the lower critical solution temperature (LCST), it exists in the form of liquid, and when the temperature exceeds the LCST, it solidifies into the gel [146]. Hydrogels have high water retention and adhesion ability. Lu et al. [147] prepared a hydrogel complex fire extinguishing agent by mixing carboxymethyl cellulose and aluminum chloride and carried out combustion inhibition experiments on LFP battery packs. The fire extinguishing time for a single battery is only 9 s, and the consumption is only 0.18 L. Hydrogel effectively reduced the height

of the flame, dispersed the flame shape, and blocked the heat transfer between batteries through kinetic energy interference, water mist diffusion, and covering cooling.
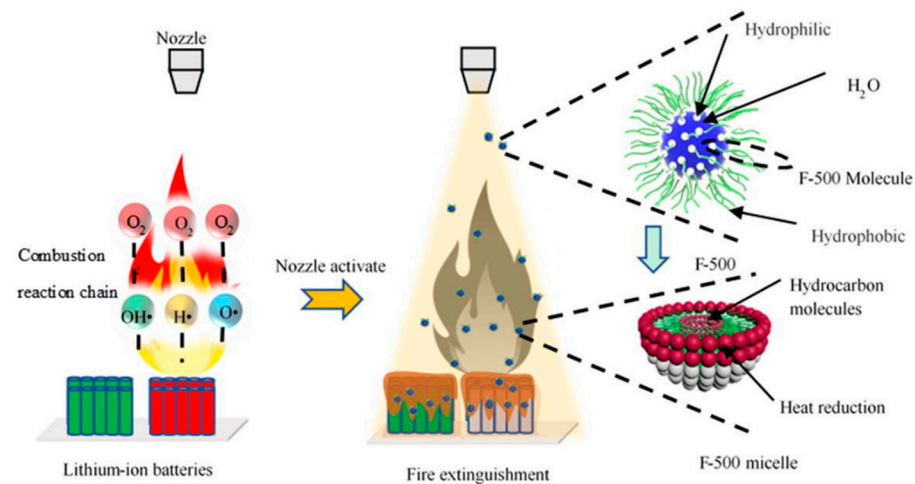
Figure 12. Mechanism of extinguishing battery fire with F500 extinguishing agent [107].

4.3.3. Foam Extinguishing Agent

Foam has high viscosity and low density, which can cover the surface of combustibles, and its main component is still water. Therefore, its extinguishing mechanism is mainly water evaporative cooling, forming a barrier on the surface of burning objects to isolate oxygen and heat [148]. Russoa et al. [149] compared the inhibition of CO_2, foam extinguishing agent, water mist, water, and dry powder extinguishing agent on LIB fire, and found that water and foam extinguishing agent might be effective in suppressing LIB fire. The comparison results are shown in Figure 13. Cui et al. [150] selected water and compressed air foam as the fire extinguishing agent to extinguish the battery pack fire, and proposed the electric vehicle fire enclosure fire extinguishing method. Their experimental results showed that 0.743 m^3/kWh of foam could inhibit the full-size LIB TR. Li et al. [151] used a 3% aqueous film-forming foam extinguishing agent to suppress 18,650 battery pack fires. The experimental results showed that although the open fire could be extinguished, it reignited 45 s later. DNV GL [129] did not recommend the use of foam extinguishing agent in the fire of energy storage stations because the battery module fire required rapid cooling to dissipate heat. Compared with water, foam had more difficulty penetrating the gap of battery packs and cooling the insides of batteries.
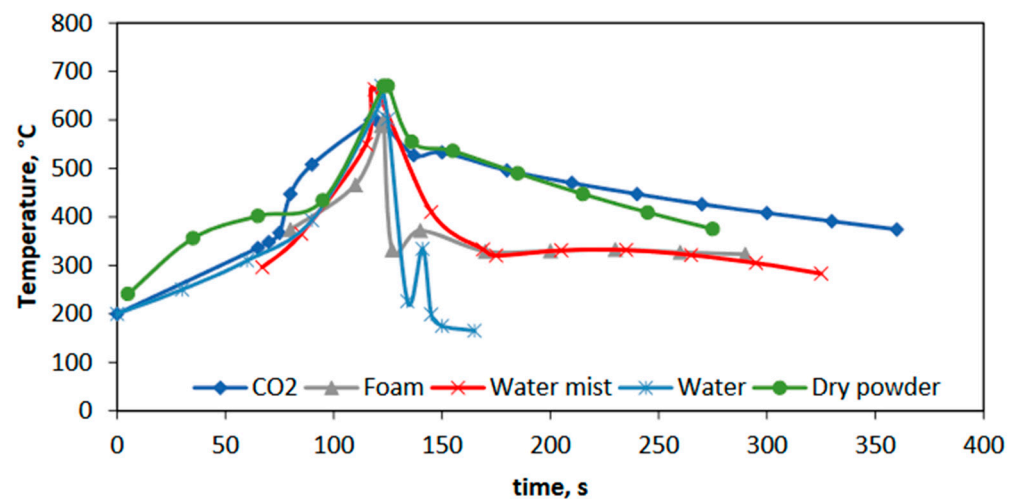
Figure 13. Extinguishing battery fire with different extinguishing agents [149].

4.3.4. Liquid Nitrogen

Liquid nitrogen has been universally applied because of its excellent cooling performance, but its application in battery firefighting is still rare. Huang et al. [152,153] first used liquid nitrogen for LIB fires, and declared that the cooling mechanism of liquid nitrogen for battery TR was mainly through membrane boiling heat transfer and radiation heat transfer. When the liquid nitrogen contacts the high-temperature surface of the battery, it will evaporate immediately, forming a layer of vapor film on the battery surface, making the liquid nitrogen droplets suspend on the battery surface. Wang et al. [154] suppressed battery TR and its propagation in confined space by injecting liquid nitrogen. The gasification of liquid nitrogen was conducive to blocking thermal convection and thermal radiation among batteries. At the same time, the gasification of liquid nitrogen into nitrogen would also absorb a lot of heat, diluted the air around the battery, and isolated oxygen. However, in engineering applications, the risk of freezing injury and asphyxiation caused by liquid nitrogen ($-196\,°C$, atmospheric pressure) should also be fully considered; namely, necessary safety protection measures must be taken.

4.3.5. Aqueous Vermiculite Dispersion

Vermiculite is a layered aluminum iron magnesium silicate mineral. The volume of vermiculite expands dozens of times at high temperature. Vermiculite is dispersed in water after grinding, forming a stable vermiculite dispersion in water. Its fire extinguishing mechanism is mainly to cool down and isolate. After release, a film is formed on the surface of LIBs and absorbs heat at a high temperature [155]. Guo et al. [156] carried out TR suppression of 21,700 LIBs by vermiculite. The results showed that aqueous vermiculite dispersion (AVD) effectively reduced the battery surface peak temperature by 71.9% and 43.8%, respectively, during the initial explosion and detonation stages of the LIBs and prevented the battery from reignition and spread. Nevertheless, AVD takes longer to extinguish the battery pack fire than other fire extinguishing agents because it is difficult for the high viscosity AVD fire extinguishing agent to penetrate the gap between batteries [157].

4.4. Comparison of Fire Extinguishing Agent

Through the analysis and comparison in Table 4, it is found that although the gas extinguishing agent can put out the open fire, the cooling effect is poor, and the possibility of TR propagation or reignition of the battery is still large. Gas extinguishing agents in confined spaces may increase system toxicity and reduce space oxygen concentration, which is more harmful to fire rescue personnel. The solid fire extinguishing agent also has an insufficient cooling effect, and it is difficult to enter the gap between the battery packs. Therefore, the suppression effect of the fire extinguishing agent is limited, and the battery will still spread or re-ignite. Dry water fire extinguishing agent combines the advantages of fine water mist and dry powder fire extinguishing agent and is the research direction of a new type of battery-efficient fire extinguishing agent. However, the liquid fire extinguishing agent may have a certain impact on the battery circuit, which may cause a short circuit of the battery. However, it has a strong cooling effect, and it is still an efficient extinguishing agent for battery fire. Proper additives can significantly improve the cooling capacity of pure water and reduce pure water consumption. Therefore, research on water-based fire extinguishing agents should focus more on low conductivity and high cooling effects. The cooling effect of liquid nitrogen is excellent; the effect of restraining TR and its propagation is good, but there is a risk of frostbite and suffocation, which should also be further studied.

Table 4. Effect of fire extinguishing agent and its advantages and disadvantages.

Category	Fire Extinguishing Agent	Extinguishing Battery Fire Effect	Advantages	Disadvantages
Gas	Halon	Good	No residue and corrosion, good insulation	Environmental pollution, damage to the ozone layer
	CO_2	Poor	No residue and corrosion, good insulation	Easy reignition, concentration leads to poisoning and asphyxia
	HFC-227ea	Medium	Low residue and corrosion	High toxicity
	Novec-1230	Good	Good cooling effect	High toxicity
	2-BTP	Good	Good cooling effect	High cost
	Aerosol	Poor	Low toxicity	Poor cooling capacity, residual and corrosive
Solid	BC dry powder	Poor	No residue and corrosion, good insulation	Poor cooling capacity, residual
	ABC dry powder	Poor	No residue and corrosion, good insulation	Poor cooling capacity, residual
	Dry water	Medium	No residue and corrosion, good insulation, medium cooling capacity	Poor pressure resistance and easy to crack
Liquid	Water mist	Good	Good cooling capacity, low price and easy access	High water consumption
	Water mist with additives	Good	Improved cooling capacity and low water consumption	High conductivity
	Hydrogel	Good	Good cooling capacity and low consumption	High viscosity, poor heat dissipation
	Foam	Poor	Low toxicity and low price	Low cooling capacity, difficult to penetrate into the battery pack gap
	Liquid nitrogen	Excellent	Excellent cooling capacity, no toxicity, no residue	Cryogenic frostbite and asphyxia
	Aqueous vermiculite dispersion	Medium	no toxicity, medium, cooling capacity	Low cooling capacity, difficult to penetrate into the battery pack gap

In conclusion, most of the previous studies focusing on the effect of fire extinguishing agent on the fire extinguishing time of batteries did not consider the optimal amount of fire extinguishing agent, the degree of battery damage, and the impact of fire extinguishing agent on the battery that is still available. Whether the battery after fire extinguishing can continue to be used, the cost of fire extinguishing, and the application in different situations should be further analyzed. Thus far, the existing fire extinguishing agent has a long duration, large consumption, short-circuit risk, easy reignition, and potential explosion risk in the fire extinguishing process, which has become a world problem that plagues the LIB's fire safety. It is urgent to develop a new type of fire extinguishing agent that is highly efficient and suitable for batteries.

5. Summary and Outlook

With the wide application of LIBs, more and more attention has been paid to their safety. In order to avoid battery TR, monitoring and early warning should be carried out, and cooling and fire extinguishing measures should be taken in time to prevent further expansion of the accident. This work analyzed the process and characteristics of battery TR, summarized the monitoring and early warning methods of battery TR from five aspects of "acoustic, heat, force, electricity and gas", reviewed the efficient extinguishing agents for LIB fires, and made the following conclusions and prospects:

(1) The characteristics of battery TR are mainly embodied in five aspects: "sound, heat, force, electricity and gas". Only by deeply understanding the characteristics and mechanism of battery TR can a reliable early warning method and efficient fire extin-

guishing technology be developed. TR tests are difficult to reproduce, especially if they are done on commercial cells/batteries, which is the most frequent case. Therefore, all experimental results have to be treated with caution, and a better standardization of TR testing is highly needed.

(2) Special early warning schemes should be provided for different types of batteries, such as soft packages and steel shells. After improving the early warning accuracy, the realization of multi-level and multi-type early warning methods complementation and interworking should be focused on. The internal early warning system of the battery should be implanted from the time of manufacture, paying attention to sensor corrosion and its impact on electrochemical performance. The external early warning system should select the best sensor layout location to improve the accuracy of the warning and reduce the system's misjudgment rate.

(3) The environmental toxicity and asphyxiation of battery fire extinguishants should be considered. The fire extinguishing agent should develop toward anti-reignition, rapid cooling, low conductivity, and improve the absorption capacity of toxic gases, flammable, and explosive gases. For LIBs fire in confined space or semi-confined space, a variety of fire extinguishing forms can be considered, such as injecting an extinguishing agent into the confined space. For different fire intensities, cooperative suppression of the extinguishing agent can be considered. At present, research on the extinguishant of LIB fire is mostly small-scale, and large-scale experimental research should be carried out.

(4) In combination with early warning and firefighting, the risk of battery TR should be graded and rapidly linked. LIBs should be graded in practical applications, and the battery monomer, battery module, battery cluster, battery pack, etc. should be graded for early warning and fire protection.

Data Availability Statement: Data are contained within the article.

Conflicts of Interest: The authors declare no conflict of interest.

References

1. Zhao, F.; Bai, F.; Liu, X.; Liu, Z. A Review on Renewable Energy Transition under China's Carbon Neutrality Target. *Sustainability* **2022**, *14*, 15006. [CrossRef]
2. Lai, X.; Yao, J.; Jin, C.; Feng, X.; Wang, H.; Xu, C.; Zheng, Y. A Review of Lithium-Ion Battery Failure Hazards: Test Standards, Accident Analysis, and Safety Suggestions. *Batteries* **2022**, *8*, 248. [CrossRef]
3. Tianyu, C.; Shang, G.; Xuning, F.; Languang, L.; Minggao, O. Recent progress on thermal runaway propagation of lithium-ion battery. *Energy Storage Sci. Technol.* **2018**, *7*, 1030.
4. Hill, D. *McMicken Battery Energy Storage System Event: Technical Analysis and Recommendations*; DNV GL Energy Insights USA, Incorporated: Dallas, TX, USA, 2020.
5. Wang, K.; Cao, Y.; Yang, Y.; Wang, Z.; Ouyang, D. Exploring fluorinated electrolyte for high-voltage and high-safety Li-ion cells with Li(Ni$_{0.8}$Mn$_{0.1}$Co$_{0.1}$)O$_2$ cathode. *Int. J. Energy Res.* **2022**, *46*, 24243–24253. [CrossRef]
6. Ouyang, D.; Wang, K.; Pang, Y.; Wang, Z. A fluorinated carbonate-based electrolyte for high-voltage Li(Ni$_{0.8}$Mn$_{0.1}$Co$_{0.1}$)O$_2$ lithium-ion cells. *J. Power Sources* **2022**, *529*, 231247. [CrossRef]
7. Ouyang, D.; Wang, K.; Pang, Y.; Wang, Z. Optimal Blend between Carbonate Solvents and Fluoroethylene Carbonate for High-Voltage and High-Safety Li(Ni$_{0.8}$Mn$_{0.1}$Co$_{0.1}$)O$_2$ Lithium-Ion Cells. *ACS Appl. Energy Mater.* **2023**, *6*, 3. [CrossRef]
8. Ouyang, D.; Wang, K.; Yang, Y.; Wang, Z. Fluoroethylene carbonate as co-solvent for Li(Ni$_{0.8}$Mn$_{0.1}$Co$_{0.1}$)O$_2$ lithium-ion cells with enhanced high-voltage and safety performance. *J. Power Sources* **2022**, *542*, 231780. [CrossRef]
9. Schadeck, U.; Kyrgyzbaev, K.; Zettl, H.; Gerdes, T.; Moos, R. Flexible, heat-resistant, and flame-retardant glass fiber nonwoven/glass platelet composite separator for lithium-ion batteries. *Energies* **2018**, *11*, 999. [CrossRef]
10. Zhang, J.; Yue, L.; Kong, Q.; Liu, Z.; Zhou, X.; Zhang, C.; Xu, Q.; Zhang, B.; Ding, G.; Qin, B. Sustainable, heat-resistant and flame-retardant cellulose-based composite separator for high-performance lithium ion battery. *Sci. Rep.* **2014**, *4*, 3935. [CrossRef]

11. Liang, Y.; Xiao, Y.; Yan, C.; Xu, R.; Ding, J.-F.; Liang, J.; Peng, H.-J.; Yuan, H.; Huang, J.-Q. A bifunctional ethylene-vinyl acetate copolymer protective layer for dendrites-free lithium metal anodes. *J. Energy Chem.* **2020**, *48*, 203–207. [CrossRef]

12. Cho, W.; Kim, S.-M.; Song, J.H.; Yim, T.; Woo, S.-G.; Lee, K.-W.; Kim, J.-S.; Kim, Y.-J. Improved electrochemical and thermal properties of nickel rich $LiNi_{0.6}Co_{0.2}Mn_{0.2}O_2$ cathode materials by SiO_2 coating. *J. Power Sources* **2015**, *282*, 45–50. [CrossRef]

13. Liu, Z.; Hu, Q.; Guo, S.; Yu, L.; Hu, X. Thermoregulating Separators Based on Phase-Change Materials for Safe Lithium-Ion Batteries. *Adv. Mater.* **2021**, *33*, 2008088. [CrossRef] [PubMed]

14. Ouyang, D.; Weng, J.; Hu, J.; Liu, J.; Chen, M.; Huang, Q.; Wang, J. Effect of high temperature circumstance on lithium-ion battery and the application of phase change material. *J. Electrochem. Soc.* **2019**, *166*, A559. [CrossRef]

15. Fayaz, H.; Afzal, A.; Samee, A.M.; Soudagar, M.E.M.; Akram, N.; Mujtaba, M.; Jilte, R.; Islam, M.T.; Ağbulut, Ü.; Saleel, C.A. Optimization of thermal and structural design in lithium-ion batteries to obtain energy efficient battery thermal management system (BTMS): A critical review. *Arch. Comput. Methods Eng.* **2022**, *29*, 129–194. [CrossRef]

16. Chen, D.; Jiang, J.; Kim, G.-H.; Yang, C.; Pesaran, A. Comparison of different cooling methods for lithium ion battery cells. *Appl. Therm. Eng.* **2016**, *94*, 846–854. [CrossRef]

17. Wang, H.; Tao, T.; Xu, J.; Mei, X.; Liu, X.; Gou, P. Cooling capacity of a novel modular liquid-cooled battery thermal management system for cylindrical lithium ion batteries. *Appl. Therm. Eng.* **2020**, *178*, 115591. [CrossRef]

18. Ouyang, D.; Chen, M.; Weng, J.; Wang, K.; Wang, J.; Wang, Z. Exploring the thermal stability of lithium-ion cells via accelerating rate calorimetry: A review. *J. Energy Chem.* **2023**, *in press*. [CrossRef]

19. Wang, Z.; Zhu, L.; Liu, J.; Wang, J.; Yan, W. Gas Sensing Technology for the Detection and Early Warning of Battery Thermal Runaway: A Review. *Energy Fuels* **2022**, *36*, 6038–6057. [CrossRef]

20. Sun, J.; Mao, B.; Wang, Q. Progress on the research of fire behavior and fire protection of lithium ion battery. *Fire Saf. J.* **2021**, *120*, 103119. [CrossRef]

21. Un, C.; Aydın, K. Thermal runaway and fire suppression applications for different types of lithium ion batteries. *Vehicles* **2021**, *3*, 480–497. [CrossRef]

22. Ouyang, D.; Wang, K.; Gao, T.; Wang, Z. Investigation on safety characteristics of high-nickel lithium-ion cells with anode partially doped by silicon oxide. *J. Loss Prev. Process Ind.* **2022**, *80*, 104924. [CrossRef]

23. Ouyang, D.; Liu, Y.; Hamam, I.; Wang, J.; Dahn, J. A comparative study on the reactivity of charged Ni-rich and Ni-poor positive electrodes with electrolyte at elevated temperatures using accelerating rate calorimetry. *J. Energy Chem.* **2021**, *60*, 523–530. [CrossRef]

24. Hou, J.; Lu, L.; Wang, L.; Ohma, A.; Ren, D.; Feng, X.; Li, Y.; Li, Y.; Ootani, I.; Han, X. Thermal runaway of Lithium-ion batteries employing $LiN(SO_2F)_2$-based concentrated electrolytes. *Nat. Commun.* **2020**, *11*, 5100. [CrossRef]

25. Wang, Q.; Mao, B.; Stoliarov, S.I.; Sun, J. A review of lithium ion battery failure mechanisms and fire prevention strategies. *Prog. Energy Combust. Sci.* **2019**, *73*, 95–131. [CrossRef]

26. Zeng, D.; Gagnon, L.; Wang, Y. Cell-level hazard evaluation of 18650 form-factor Lithium-ion battery with different cathode materials. *Proc. Combust. Inst.* **2022**, *in press*. [CrossRef]

27. Venugopal, G. Characterization of thermal cut-off mechanisms in prismatic lithium-ion batteries. *J. Power Sources* **2001**, *101*, 231–237. [CrossRef]

28. Ping, P.; Wang, Q.; Huang, P.; Li, K.; Sun, J.; Kong, D.; Chen, C. Study of the fire behavior of high-energy lithium-ion batteries with full-scale burning test. *J. Power Sources* **2015**, *285*, 80–89. [CrossRef]

29. Finegan, D.P.; Scheel, M.; Robinson, J.B.; Tjaden, B.; Hunt, I.; Mason, T.J.; Millichamp, J.; Di Michiel, M.; Offer, G.J.; Hinds, G. In-operando high-speed tomography of lithium-ion batteries during thermal runaway. *Nat. Commun.* **2015**, *6*, 6924. [CrossRef]

30. Ouyang, D.; Chen, M.; Wei, R.; Wang, Z.; Wang, J. A study on the fire behaviors of 18650 battery and batteries pack under discharge. *J. Therm. Anal. Calorim.* **2019**, *136*, 1915–1926. [CrossRef]

31. Ouyang, D.; Weng, J.; Chen, M.; Wang, J. What a role does the safety vent play in the safety of 18650-size lithium-ion batteries? *Process Saf. Environ. Prot.* **2022**, *159*, 433–441. [CrossRef]

32. Su, T.; Lyu, N.; Zhao, Z.; Wang, H.; Jin, Y. Safety warning of lithium-ion battery energy storage station via venting acoustic signal detection for grid application. *J. Energy Storage* **2021**, *38*, 102498. [CrossRef]

33. Cheng, X.; Li, T.; Ruan, X.; Wang, Z. Thermal runaway characteristics of a large format lithium-ion battery module. *Energies* **2019**, *12*, 3099. [CrossRef]

34. Chen, M.; Dongxu, O.; Liu, J.; Wang, J. Investigation on thermal and fire propagation behaviors of multiple lithium-ion batteries within the package. *Appl. Therm. Eng.* **2019**, *157*, 113750. [CrossRef]

35. Ren, D.; Feng, X.; Lu, L.; Ouyang, M.; Zheng, S.; Li, J.; He, X. An electrochemical-thermal coupled overcharge-to-thermal-runaway model for lithium ion battery. *J. Power Sources* **2017**, *364*, 328–340. [CrossRef]

36. Torabi, F.; Esfahanian, V. Study of thermal–runaway in batteries I. Theoretical study and formulation. *J. Electrochem. Soc.* **2011**, *158*, A850. [CrossRef]

37. Mier, F.A.; Hill, S.M.; Lamb, J.; Hargather, M.J. Non-invasive internal pressure measurement of 18650 format lithium ion batteries during thermal runaway. *J. Energy Storage* **2022**, *51*, 104322. [CrossRef]

38. Jhu, C.-Y.; Wang, Y.-W.; Shu, C.-M.; Chang, J.-C.; Wu, H.-C. Thermal explosion hazards on 18650 lithium ion batteries with a VSP2 adiabatic calorimeter. *J. Hazard. Mater.* **2011**, *192*, 99–107. [CrossRef]

39. Zhao, C. *Study on the Risk of Thermal Runaway Deflagration of Ternary Lithium-ion Batteries in Confined Space*; University of Science and Technology of China: Hefei, China, 2021.
40. Zhao, C.; Sun, J.; Wang, Q. Thermal runaway hazards investigation on 18650 lithium-ion battery using extended volume accelerating rate calorimeter. *J. Energy Storage* **2020**, *28*, 101232. [CrossRef]
41. Wu, M.-S.; Chiang, P.-C.J.; Lin, J.-C.; Jan, Y.-S. Correlation between electrochemical characteristics and thermal stability of advanced lithium-ion batteries in abuse tests—Short-circuit tests. *Electrochim. Acta* **2004**, *49*, 1803–1812. [CrossRef]
42. Richard, M.; Dahn, J. Predicting electrical and thermal abuse behaviours of practical lithium-ion cells from accelerating rate calorimeter studies on small samples in electrolyte. *J. Power Sources* **1999**, *79*, 135–142. [CrossRef]
43. Ouyang, D.; Weng, J.; Chen, M.; Wang, J. Impact of charging and charging rate on thermal runaway behaviors of lithium-ion cells. *J. Electrochem. Soc.* **2021**, *168*, 120510. [CrossRef]
44. Larsson, F.; Andersson, P.; Blomqvist, P.; Lorén, A.; Mellander, B.-E. Characteristics of lithium-ion batteries during fire tests. *J. Power Sources* **2014**, *271*, 414–420. [CrossRef]
45. Diaz, F.; Wang, Y.; Weyhe, R.; Friedrich, B. Gas generation measurement and evaluation during mechanical processing and thermal treatment of spent Li-ion batteries. *Waste Manag.* **2019**, *84*, 102–111. [CrossRef] [PubMed]
46. Abraham, D.; Roth, E.; Kostecki, R.; McCarthy, K.; MacLaren, S.; Doughty, D. Diagnostic examination of thermally abused high-power lithium-ion cells. *J. Power Sources* **2006**, *161*, 648–657. [CrossRef]
47. Mishra, D.; Shah, K.; Jain, A. Investigation of the impact of flow of vented gas on propagation of thermal runaway in a Li-ion battery pack. *J. Electrochem. Soc.* **2021**, *168*, 060555. [CrossRef]
48. Wang, H.; Xu, H.; Zhang, Z.; Wang, Q.; Jin, C.; Wu, C.; Xu, C.; Hao, J.; Sun, L.; Du, Z. Fire and explosion characteristics of vent gas from lithium-ion batteries after thermal runaway: A comparative study. *eTransportation* **2022**, *13*, 100190. [CrossRef]
49. Pham, M.T.; Darst, J.J.; Finegan, D.P.; Robinson, J.B.; Heenan, T.M.; Kok, M.D.; Iacoviello, F.; Owen, R.; Walker, W.Q.; Magdysyuk, O.V. Correlative acoustic time-of-flight spectroscopy and X-ray imaging to investigate gas-induced delamination in lithium-ion pouch cells during thermal runaway. *J. Power Sources* **2020**, *470*, 228039. [CrossRef]
50. Rhodes, K.; Dudney, N.; Lara-Curzio, E.; Daniel, C. Understanding the degradation of silicon electrodes for lithium-ion batteries using acoustic emission. *J. Electrochem. Soc.* **2010**, *157*, A1354. [CrossRef]
51. Davies, G.; Knehr, K.W.; Van Tassell, B.; Hodson, T.; Biswas, S.; Hsieh, A.G.; Steingart, D.A. State of charge and state of health estimation using electrochemical acoustic time of flight analysis. *J. Electrochem. Soc.* **2017**, *164*, A2746. [CrossRef]
52. Hsieh, A.; Bhadra, S.; Hertzberg, B.; Gjeltema, P.; Goy, A.; Fleischer, J.W.; Steingart, D.A. Electrochemical-acoustic time of flight: In operando correlation of physical dynamics with battery charge and health. *Energy Environ. Sci.* **2015**, *8*, 1569–1577. [CrossRef]
53. Owen, R.E.; Robinson, J.B.; Weaving, J.S.; Pham, M.T.; Tranter, T.G.; Neville, T.P.; Billson, D.; Braglia, M.; Stocker, R.; Tidblad, A.A. Operando Ultrasonic Monitoring of Lithium-Ion Battery Temperature and Behaviour at Different Cycling Rates and under Drive Cycle Conditions. *J. Electrochem. Soc.* **2022**, *169*, 040563. [CrossRef]
54. Sood, B.; Osterman, M.; Pecht, M. Health monitoring of lithium-ion batteries. In Proceedings of the 2013 IEEE Symposium on Product Compliance Engineering (ISPCE), Austin, TX, USA, 7–9 October 2013; pp. 1–6.
55. Wu, Y.; Wang, Y.; Yung, W.K.; Pecht, M. Ultrasonic health monitoring of lithium-ion batteries. *Electronics* **2019**, *8*, 751. [CrossRef]
56. Wei, Z.; Liu, C.; He, H.; Li, J.; Cao, W. A Thermal Runaway Warning Method for Lithium Ion Battery Based on Ultrasonic Guided Wave Sensor. Patent CN113533992B, 8 April 2022.
57. Appleberry, M.C.; Kowalski, J.A.; Africk, S.A.; Mitchell, J.; Ferree, T.C.; Chang, V.; Parekh, V.; Xu, Z.; Ye, Z.; Whitacre, J.F. Avoiding thermal runaway in lithium-ion batteries using ultrasound detection of early failure mechanisms. *J. Power Sources* **2022**, *535*, 231423. [CrossRef]
58. Devin Jr, C. Survey of thermal, radiation, and viscous damping of pulsating air bubbles in water. *J. Acoust. Soc. Am.* **1959**, *31*, 1654–1667. [CrossRef]
59. Lyu, N.; Jin, Y.; Miao, S.; Xiong, R.; Xu, H.; Gao, J.; Liu, H.; Li, Y.; Han, X. Fault Warning and Location in Battery Energy Storage Systems via Venting Acoustic Signal. *IEEE J. Emerg. Sel. Top. Power Electron.* **2023**, *11*, 100–108. [CrossRef]
60. Esho, I.; Shah, K.; Jain, A. Measurements and modeling to determine the critical temperature for preventing thermal runaway in Li-ion cells. *Appl. Therm. Eng.* **2018**, *145*, 287–294. [CrossRef]
61. Xu, J.; Lan, C.; Qiao, Y.; Ma, Y. Prevent thermal runaway of lithium-ion batteries with minichannel cooling. *Appl. Therm. Eng.* **2017**, *110*, 883–890. [CrossRef]
62. Lee, C.-Y.; Lee, S.-J.; Hung, Y.-M.; Hsieh, C.-T.; Chang, Y.-M.; Huang, Y.-T.; Lin, J.-T. Integrated microsensor for real-time microscopic monitoring of local temperature, voltage and current inside lithium ion battery. *Sens. Actuators A* **2017**, *253*, 59–68. [CrossRef]
63. Wang, S.; Li, K.; Tian, Y.; Wang, J.; Wu, Y.; Ji, S. Infrared imaging investigation of temperature fluctuation and spatial distribution for a large laminated lithium–ion power battery. *Appl. Therm. Eng.* **2019**, *152*, 204–214. [CrossRef]
64. Sun, L.; Sun, W.; You, F. Core temperature modelling and monitoring of lithium-ion battery in the presence of sensor bias. *Appl. Energy* **2020**, *271*, 115243. [CrossRef]
65. Parhizi, M.; Ahmed, M.; Jain, A. Determination of the core temperature of a Li-ion cell during thermal runaway. *J. Power Sources* **2017**, *370*, 27–35. [CrossRef]
66. Mutyala, M.S.K.; Zhao, J.; Li, J.; Pan, H.; Yuan, C.; Li, X. In-situ temperature measurement in lithium ion battery by transferable flexible thin film thermocouples. *J. Power Sources* **2014**, *260*, 43–49. [CrossRef]

67. Raijmakers, L.; Danilov, D.; Eichel, R.-A.; Notten, P. A review on various temperature-indication methods for Li-ion batteries. *Appl. Energy* **2019**, *240*, 918–945. [CrossRef]

68. Zhu, S.; Han, J.; An, H.-Y.; Pan, T.-S.; Wei, Y.-M.; Song, W.-L.; Chen, H.-S.; Fang, D. A novel embedded method for in-situ measuring internal multi-point temperatures of lithium ion batteries. *J. Power Sources* **2020**, *456*, 227981. [CrossRef]

69. Li, B.; Parekh, M.H.; Adams, R.A.; Adams, T.E.; Love, C.T.; Pol, V.G.; Tomar, V. Lithium-ion battery thermal safety by early internal detection, prediction and prevention. *Sci. Rep.* **2019**, *9*, 1–11. [CrossRef] [PubMed]

70. Li, B.; Parekh, M.H.; Pol, V.G.; Adams, T.E.; Fleetwood, J.; Jones, C.M.; Tomar, V. Operando Monitoring of Electrode Temperatures during Overcharge-Caused Thermal Runaway. *Energy Technol.* **2021**, *9*, 2100497. [CrossRef]

71. Nascimento, M.; Ferreira, M.S.; Pinto, J.L. Real time thermal monitoring of lithium batteries with fiber sensors and thermocouples: A comparative study. *Measurement* **2017**, *111*, 260–263. [CrossRef]

72. Yang, G.; Leitão, C.; Li, Y.; Pinto, J.; Jiang, X. Real-time temperature measurement with fiber Bragg sensors in lithium batteries for safety usage. *Measurement* **2013**, *46*, 3166–3172. [CrossRef]

73. Nascimento, M.; Ferreira, M.S.; Pinto, J.L. Temperature fiber sensing of Li-ion batteries under different environmental and operating conditions. *Appl. Therm. Eng.* **2019**, *149*, 1236–1243. [CrossRef]

74. Fleming, J.; Amietszajew, T.; McTurk, E.; Towers, D.P.; Greenwood, D.; Bhagat, R. Development and evaluation of in-situ instrumentation for cylindrical Li-ion cells using fibre optic sensors. *HardwareX* **2018**, *3*, 100–109. [CrossRef]

75. Martiny, N.; Mühlbauer, T.; Steinhorst, S.; Lukasiewycz, M.; Jossen, A. Digital data transmission system with capacitive coupling for in-situ temperature sensing in lithium ion cells. *J. Energy Storage* **2015**, *4*, 128–134. [CrossRef]

76. Yang, L.; Li, N.; Hu, L.; Wang, S.; Wang, L.; Zhou, J.; Song, W.-L.; Sun, L.; Pan, T.-S.; Chen, H.-S. Internal field study of 21,700 battery based on long-life embedded wireless temperature sensor. *Acta Mech. Sin.* **2021**, *37*, 895–901. [CrossRef]

77. Ouyang, D.; Weng, J.; Chen, M.; Wang, J. Impacts of current rates on the degradation behaviors of lithium-ion batteries under over-discharge conditions. *J. Electrochem. Soc.* **2019**, *166*, A3432. [CrossRef]

78. Ouyang, D.; Weng, J.; Liu, J.; Chen, M.; Wang, J. Influence of current rate on the degradation behavior of lithium-ion battery under overcharge condition. *J. Electrochem. Soc.* **2019**, *166*, A2697. [CrossRef]

79. Chen, M.; Ouyang, D.; Weng, J.; Liu, J.; Wang, J. Environmental pressure effects on thermal runaway and fire behaviors of lithium-ion battery with different cathodes and state of charge. *Process Saf. Environ. Prot.* **2019**, *130*, 250–256. [CrossRef]

80. Sommer, L.W.; Kiesel, P.; Ganguli, A.; Lochbaum, A.; Saha, B.; Schwartz, J.; Bae, C.-J.; Alamgir, M.; Raghavan, A. Fast and slow ion diffusion processes in lithium ion pouch cells during cycling observed with fiber optic strain sensors. *J. Power Sources* **2015**, *296*, 46–52. [CrossRef]

81. Sommer, L.W.; Raghavan, A.; Kiesel, P.; Saha, B.; Staudt, T.; Lochbaum, A.; Ganguli, A.; Bae, C.-J.; Alamgir, M. Embedded fiber optic sensing for accurate state estimation in advanced battery management systems. *MRS Online Proc. Libr.* **2014**, *1681*, 1–7. [CrossRef]

82. Hahn, M.; Buqa, H.; Ruch, P.; Goers, D.; Spahr, M.; Ufheil, J.; Novák, P.; Kötz, R. A dilatometric study of lithium intercalation into powder-type graphite electrodes. *Electrochem. Solid-State Lett.* **2008**, *11*, A151. [CrossRef]

83. Zhang, N.; Tang, H. Dissecting anode swelling in commercial lithium-ion batteries. *J. Power Sources* **2012**, *218*, 52–55. [CrossRef]

84. Zhu, S.; Yang, L.; Fan, J.; Wen, J.; Feng, X.; Zhou, P.; Xie, F.; Zhou, J.; Wang, Y.-N. In-situ obtained internal strain and pressure of the cylindrical Li-ion battery cell with silicon-graphite negative electrodes. *J. Energy Storage* **2021**, *42*, 103049. [CrossRef]

85. Zhu, S.; Yang, L.; Wen, J.; Feng, X.; Zhou, P.; Xie, F.; Zhou, J.; Wang, Y.-N. In operando measuring circumferential internal strain of 18650 Li-ion batteries by thin film strain gauge sensors. *J. Power Sources* **2021**, *516*, 230669. [CrossRef]

86. Wang, L.; Duan, X.; Liu, B.; Li, Q.; Yin, S.; Xu, J. Deformation and failure behaviors of anode in lithium-ion batteries: Model and mechanism. *J. Power Sources* **2020**, *448*, 227468. [CrossRef]

87. Sun, Y.; Lu, H.; Jin, Y. Experimental and Numerical Study on Mechanical Deformation Characteristics of Lithium Iron Phosphate Pouch Battery Modules under Overcharge Conditions. *Energy Fuels* **2021**, *35*, 15172–15184. [CrossRef]

88. Koch, S.; Birke, K.P.; Kuhn, R. Fast thermal runaway detection for lithium-ion cells in large scale traction batteries. *Batteries* **2018**, *4*, 16. [CrossRef]

89. Chen, S.; Wang, Z.; Yan, W.; Liu, J. Investigation of impact pressure during thermal runaway of lithium ion battery in a semi-closed space. *Appl. Therm. Eng.* **2020**, *175*, 115429. [CrossRef]

90. Orazem, M.E.; Tribollet, B. Electrochemical impedance spectroscopy. *N. J.* **2008**, *1*, 383–389.

91. Liu, Y.; Xie, J. Failure study of commercial LiFePO4 cells in overcharge conditions using electrochemical impedance spectroscopy. *J. Electrochem. Soc.* **2015**, *162*, A2208. [CrossRef]

92. Srinivasan, R.; Carkhuff, B.G.; Butler, M.H.; Baisden, A.C. Instantaneous measurement of the internal temperature in lithium-ion rechargeable cells. *Electrochim. Acta* **2011**, *56*, 6198–6204. [CrossRef]

93. Srinivasan, R.; Demirev, P.A.; Carkhuff, B.G. Rapid monitoring of impedance phase shifts in lithium-ion batteries for hazard prevention. *J. Power Sources* **2018**, *405*, 30–36. [CrossRef]

94. Dong, P.; Liu, Z.; Wu, P.; Li, Z.; Wang, Z.; Zhang, J. Reliable and early warning of lithium-ion battery thermal runaway based on electrochemical impedance spectrum. *J. Electrochem. Soc.* **2021**, *168*, 090529. [CrossRef]

95. Lyu, N.; Jin, Y.; Xiong, R.; Miao, S.; Gao, J. Real-time overcharge warning and early thermal runaway prediction of Li-ion battery by online impedance measurement. *IEEE Trans. Ind. Electron.* **2021**, *69*, 1929–1936. [CrossRef]

96. Feng, X.; Ouyang, M.; Liu, X.; Lu, L.; Xia, Y.; He, X. Thermal runaway mechanism of lithium ion battery for electric vehicles: A review. *Energy Storage Mater.* **2018**, *10*, 246–267. [CrossRef]

97. Zhong, G.; Mao, B.; Wang, C.; Jiang, L.; Xu, K.; Sun, J.; Wang, Q. Thermal runaway and fire behavior investigation of lithium ion batteries using modified cone calorimeter. *J. Therm. Anal. Calorim.* **2019**, *135*, 2879–2889. [CrossRef]

98. Feng, X.; Pan, Y.; He, X.; Wang, L.; Ouyang, M. Detecting the internal short circuit in large-format lithium-ion battery using model-based fault-diagnosis algorithm. *J. Energy Storage* **2018**, *18*, 26–39. [CrossRef]

99. Feng, X.; Weng, C.; Ouyang, M.; Sun, J. Online internal short circuit detection for a large format lithium ion battery. *Appl. Energy* **2016**, *161*, 168–180. [CrossRef]

100. Ouyang, M.; Zhang, M.; Feng, X.; Lu, L.; Li, J.; He, X.; Zheng, Y. Internal short circuit detection for battery pack using equivalent parameter and consistency method. *J. Power Sources* **2015**, *294*, 272–283. [CrossRef]

101. Sazhin, S.V.; Dufek, E.J.; Gering, K.L. Enhancing Li-ion battery safety by early detection of nascent internal shorts. *ECS Trans.* **2016**, *73*, 161. [CrossRef]

102. Fernandes, Y.; Bry, A.; De Persis, S. Identification and quantification of gases emitted during abuse tests by overcharge of a commercial Li-ion battery. *J. Power Sources* **2018**, *389*, 106–119. [CrossRef]

103. Essl, C.E.; Golubkov, A.W.G.; Planteu, R.P.; Rasch, B.R.; Thaler, A.T.; Fuchs, A.F. Transport of li-Ion Batteries: Early Failure Detection by Gas Composition Measurements. 2018. Available online: https://www.scipedia.com/public/Essl_et_al_2018a (accessed on 6 February 2023).

104. Larsson, F.; Andersson, P.; Blomqvist, P.; Mellander, B.-E. Toxic fluoride gas emissions from lithium-ion battery fires. *Sci. Rep.* **2017**, *7*, 1–13. [CrossRef]

105. Gerelt-Od, B.; Kim, H.; Lee, U.J.; Kim, J.; Kim, N.; Han, Y.J.; Son, H.; Yoon, S. Potential Dependence of Gas Evolution in 18,650 Cylindrical Lithium-Ion Batteries Using In-Situ Raman Spectroscopy. *J. Electrochem. Soc.* **2018**, *165*, A168. [CrossRef]

106. Liao, Z.; Zhang, J.; Gan, Z.; Wang, Y.; Zhao, J.; Chen, T.; Zhang, G. Thermal runaway warning of lithium-ion batteries based on photoacoustic spectroscopy gas sensing technology. *Int. J. Energy Res.* **2022**, *46*, 21694–21702. [CrossRef]

107. Yuan, S.; Chang, C.; Zhou, Y.; Zhang, R.; Zhang, J.; Liu, Y.; Qian, X. The extinguishment mechanisms of a micelle encapsulator F-500 on lithium-ion battery fires. *J. Energy Storage* **2022**, *55*, 105186. [CrossRef]

108. Yuan, S.; Chang, C.; Zhang, J.; Liu, Y.; Qian, X. Experimental investigation of a micelle encapsulator F-500 on suppressing lithium ion phosphate batteries fire and rapid cooling. *J. Loss Prev. Process Ind.* **2022**, *79*, 104816. [CrossRef]

109. Jin, Y.; Zheng, Z.; Wei, D.; Jiang, X.; Lu, H.; Sun, L.; Tao, F.; Guo, D.; Liu, Y.; Gao, J. Detection of micro-scale Li dendrite via H2 gas capture for early safety warning. *Joule* **2020**, *4*, 1714–1729. [CrossRef]

110. Lochbaum, A.; Kiesel, P.; Wilko, L.; Bae, C.-J.; Staudt, T.; Saha, B.; Raghavan, A.; Lieberman, R.; Delgado, J.; Choi, B. Embedded fiber optic chemical sensing for internal cell side-reaction monitoring in advanced battery management systems. *MRS Online Proc. Libr.* **2014**, *1681*, 8–13. [CrossRef]

111. Yuan, S.; Chang, C.; Yan, S.; Zhou, P.; Qian, X.; Yuan, M.; Liu, K. A review of fire-extinguishing agent on suppressing lithium-ion batteries fire. *J. Energy Chem.* **2021**, *62*, 262–280. [CrossRef]

112. Summer, S.M. *Flammability Assessment of Lithium-Ion and Lithium-Ion Polymer Battery Cells Designed for Aircraft Power Usage*; US Department of Transportation, Federal Aviation Administration: Washington, DC, USA, 2010.

113. Si, R.-j.; Liu, D.-q.; Xue, S.-q. Experimental study on fire and explosion suppression of self-ignition of lithium ion battery. *Procedia Eng.* **2018**, *211*, 629–634. [CrossRef]

114. Wang, Q.; Shao, G.; Duan, Q.; Chen, M.; Li, Y.; Wu, K.; Liu, B.; Peng, P.; Sun, J. The efficiency of heptafluoropropane fire extinguishing agent on suppressing the lithium titanate battery fire. *Fire Technol.* **2016**, *52*, 387–396. [CrossRef]

115. Hynes, R.; Mackie, J.; Masri, A. Inhibition of premixed hydrogen-air flames by 2-H heptafluoropropane. *Combust. Flame* **1998**, *113*, 554–565. [CrossRef]

116. Yujun, L.; Qiangling, D.; Ke, L.; Haodong, C.; Qingsong, W. Experimental study on fire extinguishing of large-capacity lithium-ion batteries by various fire extinguishing agents. *Energy Storage Sci. Technol.* **2018**, *7*, 1105.

117. Rao, H.; Huang, Z.; Zhang, H.; Xiao, S. Study of fire tests and fire safety measures on lithiumion battery used on ships. In Proceedings of the 2015 International Conference on Transportation Information and Safety (ICTIS), Wuhan, China, 25–28 June 2015; pp. 865–870.

118. Zhang, L.; Li, Y.; Duan, Q.; Chen, M.; Xu, J.; Zhao, C.; Sun, J.; Wang, Q. Experimental study on the synergistic effect of gas extinguishing agents and water mist on suppressing lithium-ion battery fires. *J. Energy Storage* **2020**, *32*, 101801. [CrossRef]

119. Xu, W.; Jiang, Y.; Ren, X. Combustion promotion and extinction of premixed counterflow methane/air flames by C6F12O fire suppressant. *J. Fire Sci.* **2016**, *34*, 289–304. [CrossRef]

120. Wang, Q.; Li, K.; Wang, Y.; Chen, H.; Duan, Q.; Sun, J. The efficiency of dodecafluoro-2-methylpentan-3-one on suppressing the lithium ion battery fire. *J. Electrochem. Energy Convers. Storage* **2018**, *15*, 041001. [CrossRef]

121. Liu, Y.; Duan, Q.; Xu, J.; Chen, H.; Lu, W.; Wang, Q. Experimental study on the efficiency of dodecafluoro-2-methylpentan-3-one on suppressing lithium-ion battery fires. *RSC Adv.* **2018**, *8*, 42223–42232. [CrossRef] [PubMed]

122. Liu, Y.; Duan, Q.; Xu, J.; Li, H.; Sun, J.; Wang, Q. Experimental study on a novel safety strategy of lithium-ion battery integrating fire suppression and rapid cooling. *J. Energy Storage* **2020**, *28*, 101185. [CrossRef]

123. Liu, Y.; Yang, K.; Zhang, M.; Li, S.; Gao, F.; Duan, Q.; Sun, J.; Wang, Q. The efficiency and toxicity of dodecafluoro-2-methylpentan-3-one in suppressing lithium-ion battery fire. *J. Energy Chem.* **2022**, *65*, 532–540. [CrossRef]

124. Zhou, X.; Chen, W.; Chao, M.; Liao, G. The study of thermal decomposition of 2-bromo-3, 3, 3-trifluoropropene and its fire-extinguishing mechanism. *J. Fluor. Chem.* **2013**, *153*, 101–106. [CrossRef]

125. Xu, H.; Cong, X.; Zhao, L.; Wang, X. Experimental study on extinguishing efficiency of 2-BTP on battery fires. *Fire Sci. Technol.* **2022**, *41*, 873.

126. Shen, J.; He, Y.; Wang, H.; Guo, J.; Chen, X. New Clean Fire Extinguishing Agents for Lithium Battery Fire Experiments in Civil Aviation Transportation under Variable Pressure Environment. *Sci. Technol. Eng.* **2020**, *20*, 11378–11384.

127. He, Y.; Shen, J.; Wang, H. Study on extinguishing 21700 lithium battery fire with different new clean gas extinguishing agents under low pressure. *J. Saf. Sci. Technol.* **2019**, *15*, 53–58.

128. Rohilla, M.; Saxena, A.; Tyagi, Y.K.; Singh, I.; Tanwar, R.K.; Narang, R. Condensed aerosol based fire extinguishing system covering versatile applications: A review. *Fire Technol.* **2022**, *58*, 327–351. [CrossRef]

129. Edison, C. *Considerations for ESS Fire Safety*; DNV GL: Oslo, Norway, 2017.

130. Reif, R.H.; Liffers, M.; Forrester, N.; Peal, K. Lithium Battery Safety: A look at Woods Hole Oceanographic Institution's Program. *Prof. Saf.* **2010**, *55*, 32–37.

131. Zhao, J.; Xue, F.; Fu, Y.; Cheng, Y.; Yang, H.; Lu, S. A comparative study on the thermal runaway inhibition of 18650 lithium-ion batteries by different fire extinguishing agents. *Iscience* **2021**, *24*, 102854. [CrossRef] [PubMed]

132. Meng, X.; Yang, K.; Zhang, M.; Gao, F.; Liu, Y.; Duan, Q.; Wang, Q. Experimental study on combustion behavior and fire extinguishing of lithium iron phosphate battery. *J. Energy Storage* **2020**, *30*, 101532. [CrossRef]

133. Li, H.; Hua, M.; Pan, X.; Li, S.; Guo, X.; Zhang, H.; Jiang, J. The reaction pathway analysis of phosphoric acid with the active radicals: A new insight of the fire-extinguishing mechanism of ABC dry powder. *J. Mol. Model.* **2019**, *25*, 1–12. [CrossRef]

134. Saleh, K.; Forny, L.; Guigon, P.; Pezron, I. Dry water: From physico-chemical aspects to process-related parameters. *Chem. Eng. Res. Des.* **2011**, *89*, 537–544. [CrossRef]

135. Wang, Y.; Zhu, G.; Chai, G.; Zhou, Y.; Chen, C.; Zhang, W. Experimental study on the effect of release pressure on the extinguishing efficiency of dry water. *Case Stud. Therm. Eng.* **2021**, *26*, 101177. [CrossRef]

136. Kong, L. *Design and Preparation of Dry Water Fire Extinguishing Agent and Study on Fire Extinguishing Efficiency of Lithium Battery*; Academy of Military Sciences: Beijing, China, 2021.

137. Wang, Y. *Study on Preparation, Fire Extinguishing Efficiency of Dry Water Material and its Inhibition Mechanism on Thermal Runaway of Lithium Battery*; China University of Mining and Technology: Beijing, China, 2022.

138. Cui, Y.; Liu, J. Research progress of water mist fire extinguishing technology and its application in battery fires. *Process Saf. Environ. Prot.* **2021**, *149*, 559–574. [CrossRef]

139. Liu, T.; Liu, Y.; Wang, X.; Kong, X.; Li, G. Cooling control of thermally-induced thermal runaway in 18,650 lithium ion battery with water mist. *Energy Convers. Manage.* **2019**, *199*, 111969. [CrossRef]

140. Wang, W.; He, S.; He, T.; You, T.; Parker, T.; Wang, Q. Suppression behavior of water mist containing compound additives on lithium-ion batteries fire. *Process Saf. Environ. Prot.* **2022**, *161*, 476–487. [CrossRef]

141. Zhou, Y.; Wang, Z.; Gao, H.; Wan, X.; Qiu, H.; Zhang, J.; Di, J. Inhibitory effect of water mist containing composite additives on thermally induced jet fire in lithium-ion batteries. *J. Therm. Anal. Calorim.* **2021**, *147*, 2171–2185. [CrossRef]

142. Egelhaaf, M.; Kress, D.; Wolpert, D.; Lange, T.; Justen, R.; Wilstermann, H. Fire fighting of Li-ion traction batteries. *SAE Int. J. Altern. Powertrains* **2013**, *2*, 37–48. [CrossRef]

143. Cao, X.-y.; Bi, M.-s.; Ren, J.-j.; Chen, B. Experimental research on explosion suppression affected by ultrafine water mist containing different additives. *J. Hazard. Mater.* **2019**, *368*, 613–620. [CrossRef] [PubMed]

144. Zhou, Y.; Bai, J.; Wang, Z.; Wang, J.; Bai, W. Inhibition of thermal runaway in lithium-ion batteries by fine water mist containing a low-conductivity compound additive. *J. Clean. Prod.* **2022**, *340*, 130841. [CrossRef]

145. Luo, W.-t.; Zhu, S.-b.; Gong, J.-h.; Zhou, Z. Research and development of fire extinguishing technology for power lithium batteries. *Procedia Eng.* **2018**, *211*, 531–537. [CrossRef]

146. Dai, M.; Shang, Y.; Li, M.; Ju, B.; Liu, Y.; Tian, Y. Synthesis and characterization of starch ether/alginate hydrogels with reversible and tunable thermoresponsive properties. *Mater. Res. Express* **2020**, *7*, 085701. [CrossRef]

147. Jianxin, L.; ZHANG, Y.; Chuyuan, M.; Kang, D.; Chunying, L. Study on fire-extinguishing performance of hydrogel on lithium-iron-phosphate batteries. *Energy Storage Sci. Technol.* **2022**, *11*, 2637.

148. Xu, Z.; Guo, X.; Yan, L.; Kang, W. Fire-extinguishing performance and mechanism of aqueous film-forming foam in diesel pool fire. *Case Stud. Therm. Eng.* **2020**, *17*, 100578. [CrossRef]

149. Morriello, I.; Di Bari, C.; Russo, P. Effective fire extinguishing systems for lithium-ion battery. *Chem. Eng. Trans.* **2018**, *67*, 727–732.

150. Cui, Y.; Liu, J.; Han, X.; Sun, S.; Cong, B. Full-scale experimental study on suppressing lithium-ion battery pack fires from electric vehicles. *Fire Saf. J.* **2022**, *129*, 103562. [CrossRef]

151. Li, Y.; Yu, D.; Zhang, S.; Hu, Q.; Liu, X.; Wang, J. On the fire extinguishing tests of typical lithium ion battery. *J. Saf. Environ.* **2015**, *15*, 120–125.

152. Huang, Z.; Liu, P.; Duan, Q.; Zhao, C.; Wang, Q. Experimental investigation on the cooling and suppression effects of liquid nitrogen on the thermal runaway of lithium ion battery. *J. Power Sources* **2021**, *495*, 229795. [CrossRef]

153. Huang, Z.; Zhang, Y.; Song, L.; Duan, Q.; Sun, J.; Mei, W.; Wang, Q. Preventing effect of liquid nitrogen on the thermal runaway propagation in 18650 lithium ion battery modules. *Process Saf. Environ. Prot.* **2022**, *168*, 42–53. [CrossRef]

154. Wang, Z.; Wang, K.; Wang, J.; Yang, Y.; Zhu, Y.; Bai, W. Inhibition effect of liquid nitrogen on thermal runaway propagation of lithium ion batteries in confined space. *J. Loss Prev. Process Ind.* **2022**, *79*, 104853. [CrossRef]
155. Wang, H.; Sun, Q.; Guo, J.; Xie, S.; He, Y.; Chen, X. The efficiency of Aqueous Vermiculite Dispersion fire extinguishing agent on suppressing three typical power batteries. *J. Electrochem. Energy Convers. Storage* **2021**, *18*, 020901. [CrossRef]
156. Guo, J.; He, Y.; Wang, H.; Chen, X. Research on Suppression Thermal Runaway of 21700 Lithium-ion Batteries by Aqueous Vermiculite Dispersion Agent. *J. Henan Univ. Sci. Technol. (Nat. Sci.)* **2021**, *42*, 40–47.
157. Andersson, P.; Arvidson, M.; Evegren, F.; Jandali, M.; Larsson, F.; Rosengren, M. Lion Fire: Extinguishment and mitigation of fires in Li-ion batteries at sea. *Rise Saf. Transp. Saf.* **2018**, *2018*, 77.